FOXO1/3 and PTEN Depletion in Granulosa Cells Promotes Ovarian Granulosa Cell Tumor Development

Zhilin Liu, Yi A. Ren, Stephanie A. Pangas, Jaye Adams, Wei Zhou, Diego H. Castrillon, Dagmar Wilhelm, and JoAnne S. Richards

Departments of Molecular and Cellular Biology (Z.L., Y.A.R., S.A.P., J.A., J.S.R.), Pathology and Immunology (S.A.P.), and Obstetrics and Gynecology (J.A.), Baylor College of Medicine, and Department of Experimental Radiation Oncology (W.Z.), The University of Texas M.D. Anderson Cancer Center, Houston, Texas 77030; Department of Pathology (D.H.C.), The University of Texas Southwestern Medical School, Dallas, Texas 75390; and Department of Anatomy and Developmental Biology (D.W.), Monash University, Clayton VIC 3800, Australia

The forkhead box (FOX), FOXO1 and FOXO3, transcription factors regulate multiple functions in mammalian cells. Selective inactivation of the *Foxo1* and *Foxo3* genes in murine ovarian granulosa cells severely impairs follicular development and apoptosis causing infertility, and as shown here, granulosa cell tumor (GCT) formation. Coordinate depletion of the tumor suppressor *Pten* gene in the *Foxo1/3* strain enhanced the penetrance and onset of GCT formation. Immunostaining and Western blot analyses confirmed FOXO1 and phosphatase and tensin homolog (PTEN) depletion, maintenance of globin transcription factor (GATA) 4 and nuclear localization of FOXL2 and phosphorylated small mothers against decapentaplegic (SMAD) 2/3 in the tumor cells, recapitulating results we observed in human adult GCTs. Microarray and quantitative PCR analyses of mouse GCTs further confirmed expression of specific genes (*Foxl2*, *Gata4*, and *Wnt4*) controlling granulosa cell fate specification and proliferation, whereas others (*Emx2*, *Nr0b1*, *Rspo1*, and *Wt1*) were suppressed. Key genes (*Amh*, *Bmp2*, and *Fshr*) controlling follicle growth, apoptosis, and differentiation were also suppressed. *Inhbb* and *Grem1* were selectively elevated, whereas reduction of *Inha* provided additional evidence that activin signaling and small mothers against decapentaplegic (SMAD) 2/3 phosphorylation impact GCT formation. Unexpectedly, markers of Sertoli/epithelial cells (SRY [sex determining region Y]-box 9/keratin 8) and alternatively activated macrophages (chitinase 3-like 3) were elevated in discrete subpopulations within the mouse GCTs, indicating that *Foxo1/3/Pten* depletion not only leads to GCTs but also to altered granulosa cell fate decisions and immune responses. Thus, analyses of the *Foxo1/3/Pten* mouse GCTs and human adult GCTs provide strong evidence that impaired functions of the FOXO1/3/PTEN pathways lead to dramatic changes in the molecular program within granulosa cells, chronic activin signaling in the presence of FOXL2 and GATA4, and tumor formation. **(*Molecular Endocrinology* 29: 1006–1024, 2015)**

Ovarian cancer in humans is derived primarily from epithelial cells of ovarian surface or Fallopian tube origin (1–5). Ovarian tumors that are of granulosa cell origin (granulosa cell tumor [GCT]) are less common (5% of total) in women (6, 7) but represent the most common ovarian cancer subtype in some domestic species (8).

ISSN Print 0888-8809 ISSN Online 1944-9917
Printed in USA

Received April 13, 2015. Accepted June 4, 2015.
First Published Online June 10, 2015

Abbreviations: AAM, alternative activation of macrophage; AGCT, adult GCT; AKT, v-Akt murine thymoma viral oncogene; BMP, bone morphogenic protein; CHI3L3, chitinase 3-like 3; dKO, double knockout; FOX, forkhead box; KRT8, keratin 8; GATA, globin transcription factor; GCT, granulosa cell tumor; hAGCT, human AGCT; H&E, hematoxylin and eosin; IHC, immunohistochemical; INHBB, inhibin beta B; KO, knockout; OSE, ovarian surface epithelial; PI3K, phosphoinositide 3-kinase; pSMAD2/3, phosphorylated SMAD2/3; PTEN, phosphatase and tensin homolog; qPCR, quantitative PCR; SMAD, small mothers against decapentaplegic; SOX9, SRY (sex determining region Y) box 9; tKO, triple knockout; WNT, wingless type mouse mammary tumor virus integration site family.

GCTs can also occur in the testis (9, 10). In women GCTs have been subclassified as adult or juvenile based on the onset of tumor formation, tumor cell morphology and the expression of specific genes, most notably forkhead box (FOX)L2, globin transcription factor (GATA) 4, and inhibin beta B (INHBB) (6, 11). Almost all adult GCTs (AGCTs) express 1 mutant (C134W) allele of FOXL2 (12, 13), whereas juvenile GCTs do not harbor FOXL2 mutations and the extinction of *FOXL2* expression is associated with the most aggressive tumors (14, 15). Although overexpression of mutant FOXL2 can alter the expression of a few genes (16–19) and targets aromatase in GCTs (20), the functional significance of mutant FOXL2 to GCT formation and progression remains to be clearly defined (21). Some overexpression studies provide evidence that wild-type FOXL2 can impact apoptosis, inflammation, and cholesterol metabolism (18), whereas small interfering RNA or inactivated FOXL2 studies suggest other mechanisms (16, 17). Furthermore, wild-type FOXL2 plays a critical role in determining and maintaining granulosa cell fate specification in the embryonic gonad and adult ovarian follicles, respectively, by driving ovarian development as opposed to testis development, in part, by suppressing expression of SRY (sex determining region Y) box 9 (SOX9) (22–25). Thus, FOXL2 appears to impact granulosa cell functions at distinct stages of follicle development (26–28). GATA4 and GATA6 also impact granulosa cell fate specification (11, 29), functions, proliferation and follicle formation, in part by regulating expression of FOXL2 and follistatin (29, 30). Activins (homo- and heterodimers of INHBA and INHBB) signal through the small mothers against decapentaplegic (SMAD) 2/3 pathway and when unopposed as in the *Inha* knockout (KO) mouse appear to impact GCT formation (31).

Despite the occurrence of GCTs in domestic animal and women and the poor prognosis for survival in those with advanced stage disease (21, 32), the molecular mechanisms underlying the etiology of this disease are not yet entirely clear, in part, because GCTs are rare. Furthermore, only 2 immortalized cell lines of human GCTs are available: KGN cells, which were derived from a metastatic tumor of a postmenopausal patient and represent AGCTs and COV434 cells, which were derived from a young patient and represent juvenile GCTs (6). Whether or not they are representative of most GCTs is not yet known. Recent molecular and immunohistochemical (IHC) analyses of AGCTs indicate that FOXL2 is a central transcription factor in the ovary and that with GATA4 and phosphorylated SMAD2/3 (pSMAD2/3) are likely key players in tumor growth (26–28, 33, 34). Mouse models that develop GCTs have been generated (10, 31, 35–40) and have provided important clues about factors controlling GCT formation. In particular, the wingless type mouse mammary tumor virus integration site family (WNT)/β-catenin and TGFβ/activin/SMAD pathways appear to be factors involved in GCT formation (10, 37–40), although none of the current mouse models completely recapitulate the molecular phenotype of AGCTs in women.

The FSH, IGF-1, and epidermal growth factor receptor pathways also regulate granulosa cell proliferation (41–44), in part, by activating the phosphatase and tensin homolog (PTEN)/phosphoinositide 3-kinase (PI3K) kinase pathway and phosphorylation of v-Akt murine thymoma viral oncogene (AKT) (44–48). Moreover, altered activation of the insulin-like growth factor 1 receptor and epidermal growth factor receptor pathways have been implicated in promoting adult human GCT progression (49, 50), and this might be related to elevated gonadotropins in women during the perimenopausal period when adult type GCT occur most frequently (6). Specific targets of AKT include members of FOXO family of transcription factors that are highly conserved from *Caenorhabditis elegans* to man (51–54). These factors have multiple roles in mammalian cells, including proapoptotic and tumor suppression functions that are cell and context specific (55–58). In the mammalian ovary, including mouse, human, and other species, FOXO1, like FOXL2, is expressed in granulosa cells of growing follicles (54), whereas FOXO3 is primarily elevated in luteal cells (59, 60).

Targeted inactivation of both *Foxo1* and *Foxo3* (but not either gene by itself) in murine granulosa cells leads to female infertility, abnormal follicle development and the absence of corpora lutea (61), reinforcing a central role of these factors in granulosa cell fate decisions and follicle growth. However, the granulosa cells retain expression of *Foxl2*, *Gata4*, *Cyp19a1*, and activin (*Inhba* and *Inhbb*). In addition, the *Foxo1/3* mutant mice and in vitro studies show that FOXO1 exhibits both pro- and antiapoptotic functions in growing follicles depending on its interactions with either the activin or the bone morphogenic protein (BMP) pathways, respectively (61, 62). Specifically, FOXO1 interacts with activin signaling to increase expression of genes related to follicle growth, *Amh*, *Ctgf*, and *NrOb1*. By contrast, in the presence of BMP2, FOXO1 increases proapoptotic genes, *Bcl2l11* (*Bim*), *Pdk4*, and *Jnk10* (61). Thus, FOXO1 appears to mediate the responses of granulosa cells to specific survival and stress signals. FOXO3 is also present in murine oocytes and depletion of *Foxo3* leads to global activation of primordial follicles leading to premature ovarian failure (63), indicating that FOXO3 also controls the functions of germ cells and maintains follicle quiescence. Because in human oocytes FOXO1 appears to be predominant its

loss or inactivation could be a cause of premature ovarian failure in women (64).

The tumor suppressor protein PTEN also impacts the PI3K/AKT pathway by blocking AKT activation and FOXO1/3 phosphorylation (51). As a consequence, nonphosphorylated FOXO1/3 are retained in the nucleus and are transcriptionally active. Targeted depletion of the *Pten* gene in mouse granulosa cells increases proliferation and reduces apoptosis that is associated with increased ovulation rates, elevated expression of FOXO3 and sustained presence of corpora lutea (59). Targeted depletion of *Pten* also leads to GCT formation in about 7% of the mice (37). PTEN inhibitors and AKT activators have also been shown to activate secondary follicles in culture (65, 66). Collectively, these results indicate that PTEN and the PI3K pathway impacts granulosa cell functions, including proliferation by mechanisms that include FOXO1/3 phosphorylation and activity.

Based on the key roles of FOXL2 and GATA4 in maintaining granulosa cell specification and their prominence in human AGCTs (hAGCTs) (17) combined with the oncogenic potential of depleting *Pten* and *Foxo* genes or amplifying the PI3K/AKT functions (56), we hypothesized that FOXO1, FOXO3, and PTEN control granulosa cell fate decisions and the predisposition of granulosa cells to tumor development by regulating specific signaling cascades, including those dependent on FOXL2, GATA4, and INHBB. To test this hypothesis, we generated specific mutant mouse models in which *Foxo1*, *Foxo3*, and *Pten* have been deleted selectively in granulosa cells using mice expressing either *Amhr2-Cre* or *Cyp19-Cre*.

Materials and Methods

Generation of mice

The *Foxo1*$^{f/-}$;*Foxo3*$^{f/-}$;*Amhr2*-Cre and *Foxo1*$^{f/-}$;*Foxo3*$^{f/-}$;*Cyp19*-Cre mice were generated as described previously (58, 59, 61, 67). The *Foxo1*$^{f/f}$;*Foxo3*$^{f/f}$;*Pten*$^{f/f}$;*Cyp19*-cre mice were derived by crossing the *Foxo1*$^{f/f}$;*Foxo3*$^{f/f}$;*Cyp19*-cre mice with previously reported *Pten*$^{f/f}$ mice (68). Because no significant differences in ovarian morphology or gene expression patterns were noted between the *Foxo1*$^{f/-}$;*Foxo3*$^{f/-}$;*Amhr2*-cre and *Foxo1*$^{f/-}$;*Foxo3*$^{f/-}$;*Cyp19*-cre mice, the data have been pooled and the mice designated as *Foxo1/3* double knockout (dKO) unless otherwise specified. *Foxo1*$^{f/-}$;*Foxo3*$^{f/-}$ littermates lacking Cre recombinase were used as controls. All genotyping protocols follow those published in the original papers (58, 59, 61, 67). Animals were housed under a 12-hour light, 12-hour dark cycle schedule in the Center for Comparative Medicine at Baylor College of Medicine and provided food and water ad libitum. Animals were treated in accordance with the National Institutes of Health Guide for the Care and Use of Laboratory Animals, as approved by the Animal Care and Use Committee at Baylor College of Medicine.

Human AGCTs

Anonymized hAGCT specimens from women 36–61 years of age were obtained as tissue sections from archival paraffin-embedded tissue blocks (and thus in a manner exempt from full internal review board review). Sections (5 μm) of the formalin-fixed paraffin-embedded samples were prepared and used for histological and IHC analyses.

Ovarian histology

Mouse ovaries were collected, fixed in 4% paraformaldehyde and embedded in paraffin and 5-μm sections prepared. Mouse and human sections were stained with hematoxylin and eosin (H&E) by routine procedures (59). IHC and immunofluorescence analyses were done with the antibodies specific for FOXO1 (2880), PTEN (9559), and pSMAD2/3 (3101) (Cell Signaling), and collagen IV (ab6586; Abcam) as described previously (59, 62) and as presented in the figures. The SOX9 antibody (AB5535) was obtained from EMD Millipore. The anti-FOXL2 antibody was generated by Dagmar Wilhelm (Monash University, Melbourne, Australia) (69). For costaining with SOX9, a FOXL2 antibody (ab5096) from Abcam was used. The anti-chitinase 3-like 3 (CHI3L3)/YM1 antibody (01404) was obtained from StemCell Research, and the anti-keratin 8 (KRT8) (TROMA-I) antibody was obtained from the Developmental Studies Hybridoma Bank (The University of Iowa, Iowa City, Iowa) as described previously. Digital images were captured using a Zeiss AxioPlan2 Microscope with ×4, ×10, or ×20 objectives in the Integrated Microscopy Core at Baylor College of Medicine.

Hormone assays

Mouse serum samples was prepared using BD Microtainer Plastic Capillary Blood Collectors (Thermo Fisher Scientific, Inc). LH, FSH, estradiol, testosterone, inhibin A, and inhibin B levels were measured using specific assays in the Ligand Assay Core Laboratory (The University of Virginia, Center for Research in Reproduction).

RNA isolation, microarray analyses, and quantitative PCR (qPCR)

Total RNA was isolated from ovaries (or ovarian tumors) and pituitaries of control and mutant mice using the RNeasy Mini kit (QIAGEN Sciences). Reverse transcription was done using the mouse-murine leukemia virus reverse transcriptase (Promega Corp). For the microarray analyses, ovarian tumor RNA quality was assessed, and then riboprobes were generated from control and mutant RNA and hybridized to Mouse 430.2 microarray chips (Affymetrix) in the Microarray Core Facility of the Baylor College of Medicine. Microarray data were analyzed as previously reported using the Robust Multiarray Averaging function (70) from the Affy package (v1.5.8) through the BioConductor software (71). The microarray data have been deposited to gene ontology with the accession number GSE67662. http://www.ncbi.nlm.nih.gov/geo/query/acc.cgi?token=kbyfiioydzgfvcj&acc=GSE67662 This dataset was then compared with our previous datasets from granulosa cells isolated from immature mice at day 25 of age (GSE35593) (heat

map, Supplemental Table 1). The average fold differences in RNA were imported into Ingenuity Systems and analyzed using the tools provided in the Ingenuity program. qPCR was performed to verify the relative expression of granulosa cells specific genes and selected ones identified on the microarray using the Rotor-Gene 6000 thermocycler (QIAGEN Sciences) with primers for specific mRNAs designed using software Primer3 (72). Relative levels of mRNAs were calculated using Rotor-Gene 6.0 software and normalized to the levels of endogenous ribosomal protein L19 mRNA in the same samples.

Statistics

All the data were analyzed by unpaired 2-tail Student's *t* test unless specified in the figure legend. $P \leq .05$ was considered significant. Data shown were mean ± SE.

Results

Depletion of *Foxo1* and *Foxo3* expression in granulosa cells promotes ovarian GCT development

Previously, we reported conditional knockout mouse models *Foxo1*$^{f/-}$;*Foxo3*$^{f/-}$;*Amhr2*-cre and *Foxo1*$^{f/-}$;*Foxo3*$^{f/-}$;*Cyp19*-cre mice in which the *Foxo1* and *Foxo3* genes were inactivated selectively in ovarian granulosa cells using mice expressing *Amhr2-Cre* and *Cyp19-Cre* (61). These mice were sterile, exhibited impaired follicular development as well as impaired apoptosis and provided evidence that FOXO1/3 interact with both the activin and BMP2 pathways to control proliferation vs apoptosis (61).

In these studies we observe that large GCTs developed in about 20% of the *Foxo1/3* dKO mice by 6–8 months age (Figure 1A). Nine of the mice had unilateral tumors matching the 90% occurrence of unilateral GCT in women (8). Two of the mice had bilateral tumors. The tumor-bearing mice exhibited elevated levels of serum inhibin A and inhibin B (Figure 1B), a characteristic of adult human ovarian GCT patients (6). As a consequence, serum FSH and LH levels were below the level of detection (Figure 1B), and pituitary expression of *Fshb* and *Lhb* mRNA was significantly lower than in control mice (Figure 1C). Given the high serum inhibin levels, we analyzed the expression levels of the 3 subunits: *Inha*, *Inhba*,

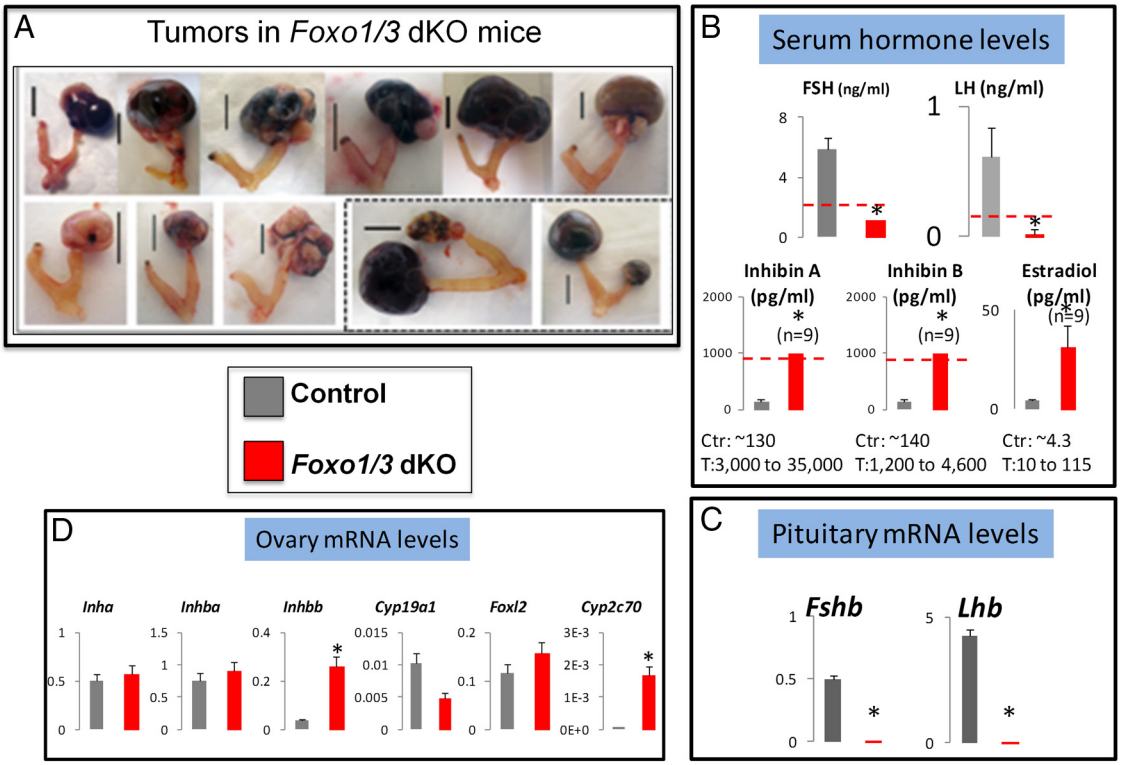

Figure 1. GCTs develop in the *Foxo1/3* dKO mice. A, *Foxo1*$^{f/-}$;*Foxo3*$^{f/-}$;*Amhr2*-Cre and *Foxo1*$^{f/-}$;*Foxo3*$^{f/-}$;*Cyp19*-Cre mice develop large unilateral (n = 8) and occasionally bilateral (n = 2, lower right) GCTs at 6–11 months of age. Most are solid; some are also cystic and hemorrhagic. B, In the *Foxo1/3* dKO mice (red bars) serum levels of FSH and LH were below the level of detection (red dashed line), whereas levels of inhibin A, inhibin B, and estradiol were elevated markedly ($P < .001$) in the tumor-bearing mice compared with control mice at 6–11 months of age (level of detection indicated by the red dashed line). C, Pituitaries from the tumor-bearing mice expressed low levels of *Fshb* and *Lhb* mRNA compared with controls (n = 9; $P < .001$), confirming the low serum levels of these hormones. Expression levels of *Inha*, *Inhba*, *Cyp19a1*, and *Foxl2* mRNAs in the tumors was similar that in control ovaries, whereas *Inhbb* and *Cyp2c70* were elevated significantly (n = 9; $P < .05$). All mRNA data are expressed relative to that encoding the ribosomal protein 19.

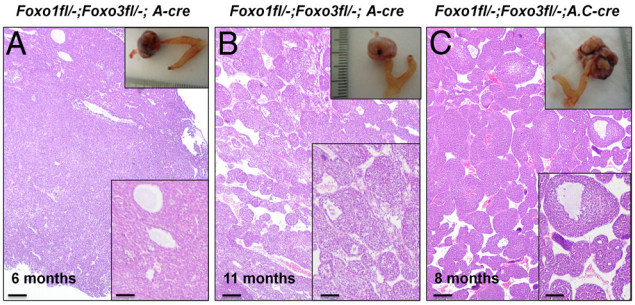

Figure 2. Histological features of the GCTs in the *Foxo1/3* dKO mice. Representative H&E 5-μm tissue sections of tumors obtained the *Foxo1*$^{fl-}$;*Foxo3*$^{fl-}$;*Amhr2*-Cre and *Foxo1*$^{fl-}$;*Foxo3*$^{fl-}$;*Amhr2-Cyp19* Cre mice at 6, 11, and 8 months of age are shown. These tumors are either olid (left panel) or exhibit trabecular-like regions (middle and right panels). Scale bars, 200 μm (A–C) and 100 μm (insets in A–C).

and *Inhbb* mRNAs in tumor cells. Interestingly, the expression levels of *Inha* or *Inhba* mRNA did not differ (Figure 1D). However, there was a 3-fold increase in *Inhbb* mRNA. Despite the low levels of FSH and LH, serum levels of estradiol were also elevated and likely reflect tumor size, because the tumors expressed lower levels *Cyp19a1* mRNA levels (Figure 1, B and D). The GCTs also expressed *Foxl2* mRNA at a level similar to that observed in control granulosa cells (Figure 1D). *Cyp2c70*, a gene we previously identified to be highly up-regulated in the *Foxo1/3*-depleted granulosa cells (61), was higher in the tumors compared with normal granulosa cells (Figure 1D). Thus, *Foxo1/3* depletion in ovarian granulosa cells leads to the development of GCTs that share some similarities with human ovarian GCTs in terms of presentation, expression of *Foxl2*, high levels of activin and inhibin and elevated estradiol. These results suggest that the *Foxo1/3* dKO mice can serve as a model for adult human GCTs.

Most tumors in the *Foxo1/3* dKO mouse from 6–11 months of age were unilateral and solid with regions of trabecular- and gyriform-like structures similar to those in AGCTs in women (Figure 2) (73). Evidence of Call-Exner bodies (fluid filled spaces between granulosa cells that recall follicular antra) was not obvious (74, 75). Some tumors also contained visible cystic or hemorrhagic follicle-like structures devoid of oocytes and/or regions of necrosis (data not shown). A few small, primary follicles and primordial follicles were also observed at the periphery of some tumor-bearing ovaries. With the exception of Call-Exner bodies, these morphological features appear similar to those observed in adult human ovarian GCTs (76). IHC analyses were performed to verify the cellular expression and localization as well as depletion of FOXO1 in tumor-bearing ovaries vs control, respectively. IHC analyses were also performed to determine the expression levels of 1) PTEN, an upstream component of the PI3K pathway and potential oncogene; 2) FOXL2, a selective marker of granulosa cells; and 3) pSMAD2/3, to assess the activation of the activin/TGFβ pathway. Because the transcription factor SOX9 is elevated in some human ovarian cancers (77, 78) but is not normally expressed in granulosa cells, we also analyzed the cellular expression of SOX9.

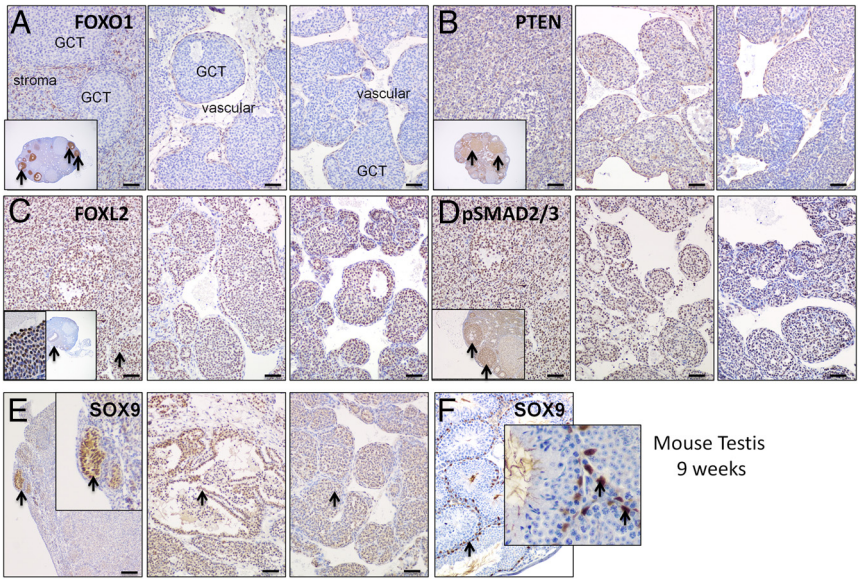

Figure 3. IHC localization of FOXO1, PTEN, FOXL2, pSMAD2/3, and SOX9 in the *Foxo1/3* dKO GCTs. Each panel represents immunostaining for a specific protein in the tumors shown in Figure 2; the insets show staining for the protein in a representative control ovary. A, Immunostaining of FOXO1 is low/absent from the granulosa cells of the 3 tumors compared with that in growing follicles of the control ovary (inset, black arrows). B, Most tumor cells are immuno-positive for PTEN, whereas in the control ovary, PTEN is most highly expressed in the stroma and corpora lutea (inset, black arrows). C, Tumor granulosa cells but not stromal elements are immuno-positive for FOXL2 as is observed in the control ovary (inset, black arrows). D, Most tumor granulosa cells are also positive for pSMAD2/3 as is also observed in the control ovary (inset, black arrows). E, Specific granulosa cells in the tumors were immuno-positive for SOX9; some positive cells were in testicular tubule-like structures (left panel, black arrows), others were in cystic-like and trabecular regions (black arrows). SOX9 positive Sertoli cells in a 9-week-old mouse testis were used as a control (black arrows). Scale bars, 50 μm (A–D and F) and 100 μm (E).

As expected, granulosa cells within the tumors exhibited negligible FOXO1 labeling compared with the intense staining of FOXO1 in granulosa cells of growing follicles in control mice (Figure 3A, inset left, black arrows). However, FOXO1 was present in stromal and vascular components of the tumors. PTEN

staining which is normally low in granulosa cells compared with luteal cells in the control ovary (Figure 3, A and B, inset, black arrows) was evident in most but not all of the tumor granulosa cells as well as in stromal, and vascular cells. By contrast, FOXL2, which is high in granulosa cells of growing follicles (Figure 3C, insets, black arrows), was selectively and intensely expressed in nuclei of the tumor granulosa cells but was clearly absent from surrounding stromal cells. The expression of FOXL2 in the tumors is consistent with the retention of granulosa cell identity; it also likely contributes to tumor formation and progression in this model (28). The tumor granulosa cells also exhibited intense nuclear pSMAD2/3 immunostaining as is observed in granulosa cells of growing follicles in control mice (Figure 3D, inset, black arrows), indicating that the activin/TGFβ pathway is active in these cells despite the presence of inhibin. pSMAD1/5 was not detected (data not shown). Quite strikingly, SOX9 (which is not present in normal granulosa cells; data not shown) was present in nuclei of granulosa cells of some follicle-like structures that had clearly lost the oocyte and in nuclei of many tumor granulosa cells localized within tubular structures (Figure 3E, inset). Because SOX9 is a marker of Sertoli cell identity (79) and epithelial cells of the Fallopian tube and endometrium (77, 78), the presence of SOX9 provides evidence that altered cell fate decisions occur in a subset of tumor cells. The mouse testis was used as a positive control (Figure 3F, black arrows).

Ovaries of younger *Foxo1/3* dKO mice at 3–4 months of age typically contained many small abnormal follicles in which fragmented oocytes or only remnants of the zona pellucida were evident (Figure 4A, left and middle panels, black arrows). The ovaries also typically contained large cyst-like structures, some of which were hemorrhagic. This is relevant, because GCTs in women can also be cystic (73). Furthermore, structures with apparent (testicular?)-tubular-like morphology were also present (Figure 4A, right panel, black arrow). FOXO1 was depleted in granulosa cells of most follicles in these ovaries, whereas PTEN appeared to be elevated in some (Figure 4B and Supplemental Figure 1). FOXL2 and phospho-SMAD2/3 (pSMAD2/3) were highly evident in the granulosa cells of small follicles and those within the cysts (Figure 4B and Supplemental Figure 1). SOX9 was present in specific structures that appeared to be derived from follicles but had (testicular?)-tubular-like morphology (Figure 4B and Supplemental Figure 1). Thus, follicular development is severely impaired in the *Foxo1/3* KO mice and is associated with large cyst-like structures and aberrant expression of SOX9.

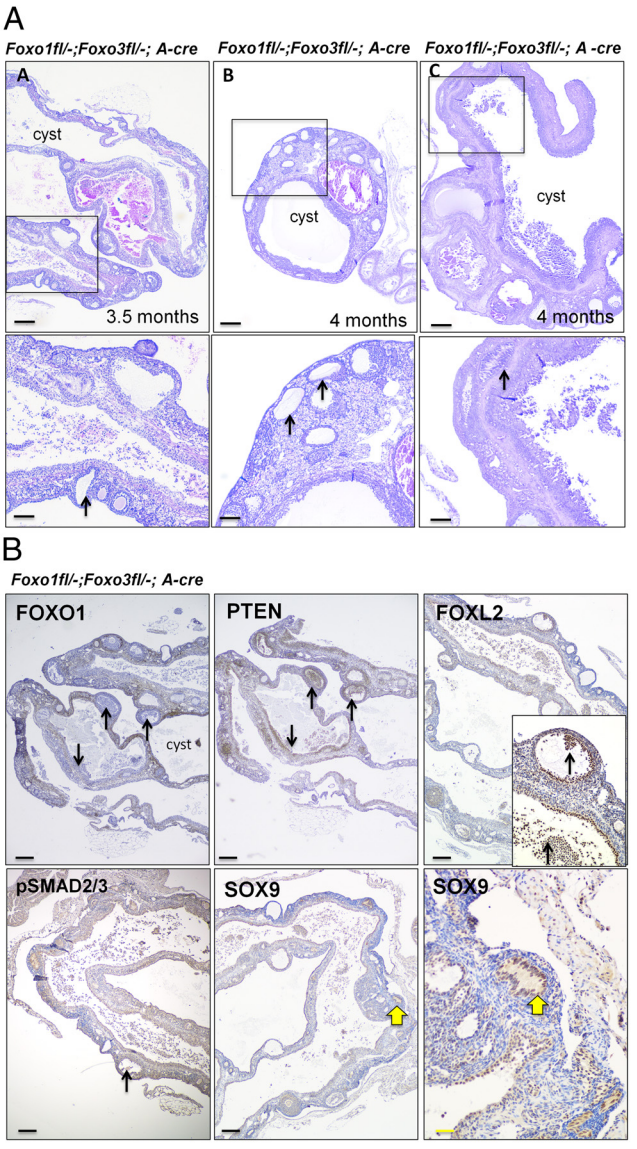

Figure 4. A, Histological features of follicles and cysts present in the *Foxo1/3* dKO mice at 3.5–4 months of age. Representative H&E 5-μm tissue sections of ovaries obtained the *Foxo1*$^{f/-}$;*Foxo3*$^{f/-}$;*Amhr2*-Cre mice at 3.5–4 months of age. a–c, All ovaries contain cysts of different sizes, some of which are also hemorrhagic. a and b, The ovaries also contain many abnormal small follicles in which the oocyte has degenerated, only remnants of the zona remain and only a few granulosa cells are present at the periphery (black arrows). c, In addition, follicles that have assumed the appearance of testicular-like structures are also evident (lower right, black arrow). Scale bars, 100 μm (a–c upper) and 200 μm (a–c lower). B, Immunolocalization of FOXO1, PTEN, FOXL2, pSMAD2/3, and SOX9. Immunostaining was performed on the ovaries from the *Foxo1/3* dKO mice at 3.5–4 months of age as shown in a (and b and c; Supplemental Figure 1): FOXO1is absent from granulosa cells in the abnormal follicles (left panel, black arrow) and those lining the cysts (middle and right panels, black arrows). PTEN is present in the granulosa cells of follicles and of the cysts (black arrows). FOXL2 is present in granulosa cells of follicles and in granulosa cells lining the large cysts (black arrows). pSMAD2/3 is also present in granulosa cells of follicles and in granulosa cells lining the large cysts (black arrows). SOX9 is observed in specific follicular structures some of which resemble testicular tubules (yellow arrows). Scale bars, 200 μm (black) and 40 μm (yellow).

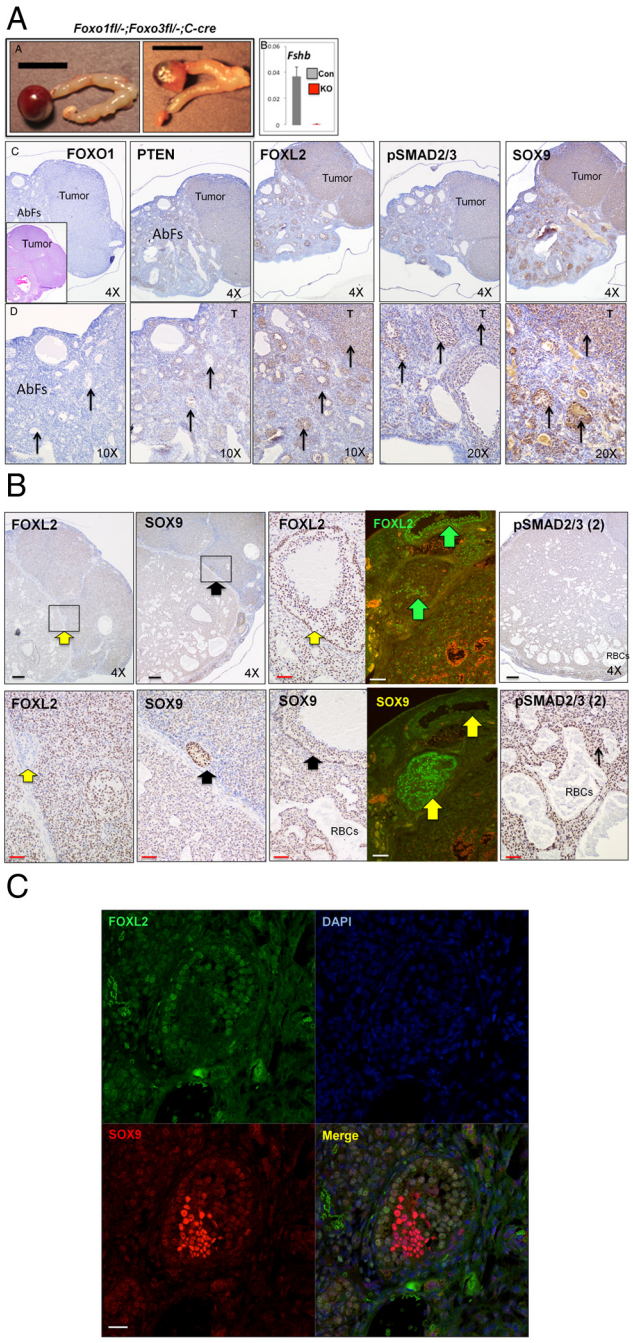

Figure 5. A, Gonadotropins enhance GCT formation in the *Foxo1/3* dKO mice. Six-week-old mice (n = 8) were injected with a superovulatory regimen of equine gonadotropin (4 IU) followed by human gonadotropin 4 IU and euthanized 1 month later. Five mice developed large GCTs by 2.5 months of age. a, Unilateral tumors in 2 representative mice are shown. b, Pituitary expression of *Fshb* mRNA in the hormone-treated *Foxo1/3* dKO markedly reduced compared with controls, as was observed in the older *Foxo1/3* dKO tumor-bearing mice (Figure 1C). c and d, FOXO1 was not detected in the granulosa cells of the solid tumor (tumor, upper panel) or granulosa cells of small abnormal follicles (AbFs) (black arrows, lower panel), whereas PTEN, FOXL2, pSMAD2/3, and SOX9 were positive in the tumor cells (T, tumor) and the granulosa cells of AbFs (black arrows). B, Localization patterns of FOXL2 and SOX9 in the gonadotropin-treated *Foxo1/3* dKO mice. Immunostaining of a more central region of the ovary shown in A shows FOXL2 and SOX9 localized to distinct structures. One small follicle-like structure is clearly FOXL2 negative (yellow arrows) but SOX9 positive (black arrows, left panels). Other follicle-like structures express both FOXL2 and SOX9 (center panels; yellow and black arrows). Immunofluorescence imaging of another section shows one follicle that is FOXL2 positive and SOX9 negative (yellow arrows) and another that contains many SOX9 positive cells and only a few FOXL2 positive cells (green arrows). The orange fluorescence is from red blood cells (RBCs). This more central region of the ovary is also filled with a trabecular-like structure that is highly vascularized and expresses pSMAD2/3 (right panels, black arrow). RBCs are evident in the highly vascularized areas. Scale bars: 200 μm (black), 40 μm (red), and 50 μm (white). C, Colocalization of FOXL2 and SOX9 in follicles of *Foxo1/3* dKO mice. Additional sections from the gonadotropin-treated mouse were costained with FOXL2 (Abcam) and SOX9 (EDM Millipore). The results show a follicle in transition from being FOXL2 positive to SOX9 positive; some cells at the periphery show low staining of both. Scale bar, 20 μm (white).

Gonadotropins increase the occurrence and onset of GCT formation in the *Foxo1/3* dKO mice

Adult GCTs occur most frequently in women during the peri- and postmenopausal years when the number of oocytes is dramatically reduced and gonadotropins are elevated suggesting that gonadotropins might impact the onset of GCT formation in women at this time. Because FSH levels are low in the *Foxo1/3* KO mice, we hypothesized that the lack of FSH might contribute to the relatively low incidence of GCT formation in these mice. Therefore, we tested whether exogenous gonadotropin treatment could increase the penetrance of GCT development in *Foxo1/3* mutant mice. To test this, 1.5-month-old *Foxo1*$^{f/-}$;*Foxo3*$^{f/-}$;*Cyp19*-cre mice in which *Fshr* mRNA is expressed at levels similar to control mice and control mice (n = 8) were injected once with superovulatory levels of equine gonadotropin (5 IU) and human gonadotropin (4 IU). Ovaries were collected 1 month later. As hypothesized, ovaries of more mutant mice (5 out of the 8; 62%) developed GCTs or cysts (Figure 5Aa), compared with those of control mice (with no Cre). Pituitary FSH expression remained lower in the *Foxo1/3* dKO mice than in control mice treated with gonadotropins and the gross morphological appearance of these earlier onset tumors was similar to that in tumors that developed later in the untreated *Foxo1/3* dKO mice at 6–9 months of age (Figure 5Ab). The GCTs lacked FOXO1 but showed immunostaining for PTEN, FOXL2, and pSMAD2/3 (Figure 5Ac). The ovaries also contained many abnormal, degenerating follicles in which the oocytes were shrunken or absent. In some follicles, granulosa cells were abnormally displaced and growing on one side. (Figure 5Ac). The granulosa cells in these abnormal (pretumorous?) structures and tumors lacked FOXO1 but were immune-positive for PTEN, FOXL2, and pSMAD2/3. The granulosa cells of some abnormal follicles also express SOX9 (Figure 5A, c and d). These features are suggestive of rapid

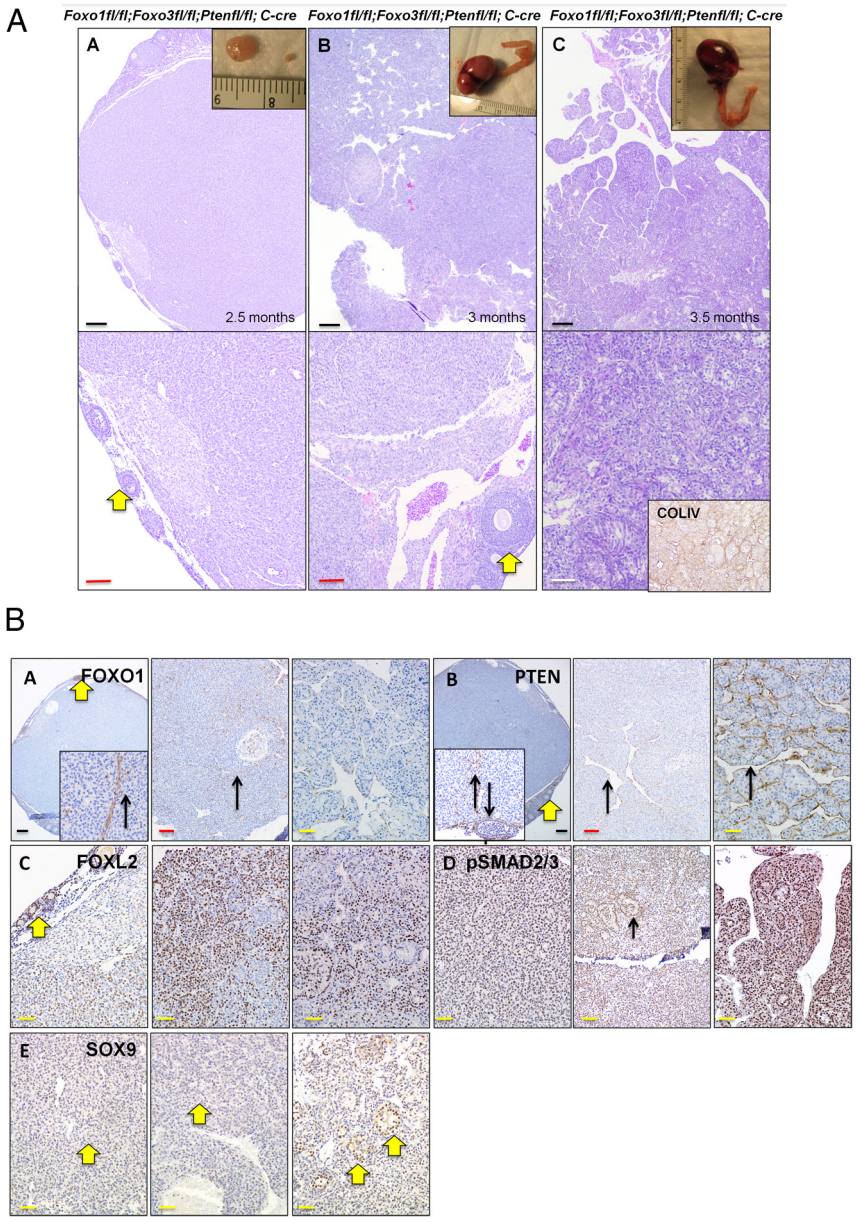

Figure 6. A, *Foxo1/3/Pten* tKO mice develop large GCTs by 2–3 months. Representative GCTs from the *Foxo1/3/Pten* tKO mice are presented. a, A solid tumor is surrounded ovarian tissue that contains small abnormal follicles, most of which have lost the oocyte. b, This large tumor contains regions that are highly trabecular. On one surface, a few primary follicles with oocytes are observed. c, This large tumor contains regions that appear trabecular and tubular, some of which resemble testicular tubules. Immunostaining of collagen IV (COLIV) shows the elaborate vascular network within the tumor (tumor tissue from a and b were used for the microarray analyses) (Figure 7). Scale bars: 200 μm (black), 80 μm (red), and 40 μm (white). B, Immunolocalization of FOXO1, PTEN, FOXL2, pSMAD2/3, and SOX9. Immunostaining was performed on ovaries of the *Foxo1/3/Pten* tKO mice at 2–3 months of age shown in A. a and b, FOXO1 staining is positive in granulosa cells of a small follicle on the periphery of the ovary (yellow arrow), whereas PTEN is positive in the theca/stromal components in the ovarian tissue (yellow arrow). FOXO1and PTEN are not expressed in the granulosa cells of the tumors but are evident in stromal and vascular components of the tumors (black arrows). c and d, FOXL2 and pSMAD2/3 are expressed in the granulosa cells of the abnormal small follicles (insets, yellow arrows) and the granulosa cells of the tumors (black arrows, insets). e, SOX9 staining is evident in the granulosa cells of the tumors and is intense is specific nests of cells (yellow arrows). Scale bars: 200 μm (black), 80 μm (red), and 40 μm (yellow).

follicle depletion in the gonadotropin treated *Foxo1/3* dKO mice as well as the abnormal (coincident?) expression of FOXL2 and SOX9 within some but not all follicles. Tissue sections obtained from a more central region of the tumor contained webs of tumor cells that were FOXL2, SOX9, and pSMAD2/3 positive (Figure 5B) that were highly vascularized or hemorrhagic. In addition, there were structures that 1) were selectively negative for FOXL2 (left panels, yellow arrows) but were positive for SOX9 (second panels, black arrows), 2) were positive for both FOXL2 and SOX9 (middle panel, yellow and black arrows or 3) contained structures in which some cells were FOXL2 positive and others appear SOX9 positive (IF, green arrows). Costaining with FOXL2 and SOX9 showed colocalization in cells at the periphery of a follicle with intense staining of only SOX9 in specific cells (Figure 5C). Thus, gonadotropins dramatically change follicle and tumor morphology and enhance tumor development in the *Foxo1/3* dKO mice associated with cell fate changes in the expression of FOXL2 and SOX9.

PTEN depletion enhances the GCT occurrence in FOXO depletion mice

Based on our observations that 1) PTEN is present in the *Foxo1/3*-depleted granulosa cells (Figure 3), 2) selective depletion of *Pten* gene in mouse granulosa cells leads to late development of GCTs in approximately 7% of the mice (37), and 3) the FOXO transcription factors are downstream of AKT in the PI3K pathway (51, 56), we next tested whether depletion of PTEN would enhance or alter the *Foxo1/3* GCT phenotype, development, and/or incidence. For this we generated *Foxo1*$^{f/f}$;*Foxo3*$^{f/f}$; *Pten*$^{f/f}$;*Cyp19*-cre mice. The triple mutant mice exhibit

a significantly higher incidence of GCT occurrence (~60%), the tumors developed earlier and most were more than 1cm^3 in size at 2–3 months of age (Figure 6A). As in the *Foxo1/3* dKO mice, serum levels of FSH and LH were below the limit of detection reflecting suppressed pituitary expression of *Fshb* and *Lhb* mRNA. Serum inhibin A and inhibin B were elevated reflecting increased expression of tumor *Inhba* and *Inhbb* but not *Inha* mRNAs. *Foxl2* expression was not different from controls but *Cyp19a1* and *Cyp2c70* levels were elevated (data not shown).

Importantly, we had previously shown that mice with conditional deletion of *Pten* alone (*Pten$^{f/f}$;Cyp19-cre*) in granulosa cells did not or rarely develop GCTs (37, 59). To exclude the possibility that *Pten* deletion may not have been efficient in this model, we generated heterozygous, germ-line depletion of *Pten* (*Pten$^{f/-}$;Cyp19-Cre*) (80) with a strategy described previously (81). Most of the *Pten$^{f/-}$;Cyp19-cre* mice are viable and fertile; only one mouse (1%) developed ovarian GCT. Thus, depletion of *Pten* in the *Foxo1/3* dKO strain clearly has a synergistic effect leading to increased incidence of tumor formation and enhanced tumor growth.

GCTs in the *Foxo1/3/Pten* triple knockout (tKO) mutant mice were either solid and surrounded by a thin layer of ovarian tissue containing a few growing follicles (Figure 6Aa) or were larger and more similar to those in ovaries of the *Foxo1/3* dKO mutant mice at 6–11 months of age (Figure 6A, b and c). In particular, the large tumors contained tubular-like structures of different sizes and shapes surrounded by a basal lamina of collagen IV (Figure 6A, b and c, inset); normal follicles were rarely observed at the periphery (Figure 6A, yellow arrows) and some of these were FOXO1 positive (Figure 6B, yellow arrow). The granulosa cells within the tumors did not express either FOXO1 or PTEN but these proteins were evident in vascular/stromal elements (Figure 6B, insets, black arrows). Granulosa cells in small growing follicles and most of the tumor cells were immunopositive for FOXL2 and pSMAD2/3, indicating that they are likely derived from granulosa cells and are responding to the activin/TGFβ signaling pathway (Figure 6B, c and d). Furthermore, SOX9 was present in the GCTs and more cells were positive in specific regions of some tumors (Figure 6Be). Large GCTs also developed early in the *Foxo1/3/Pten* tKO mutant mice treated with gonadotropins at 6 weeks of age and exhibited IHC staining patterns for FOXO1, PTEN, FOXL2, pSMAD2/3, and SOX9 similar to that of the *Foxo1/3* dKO mutant mice (Supplemental Figure 1, A and B).

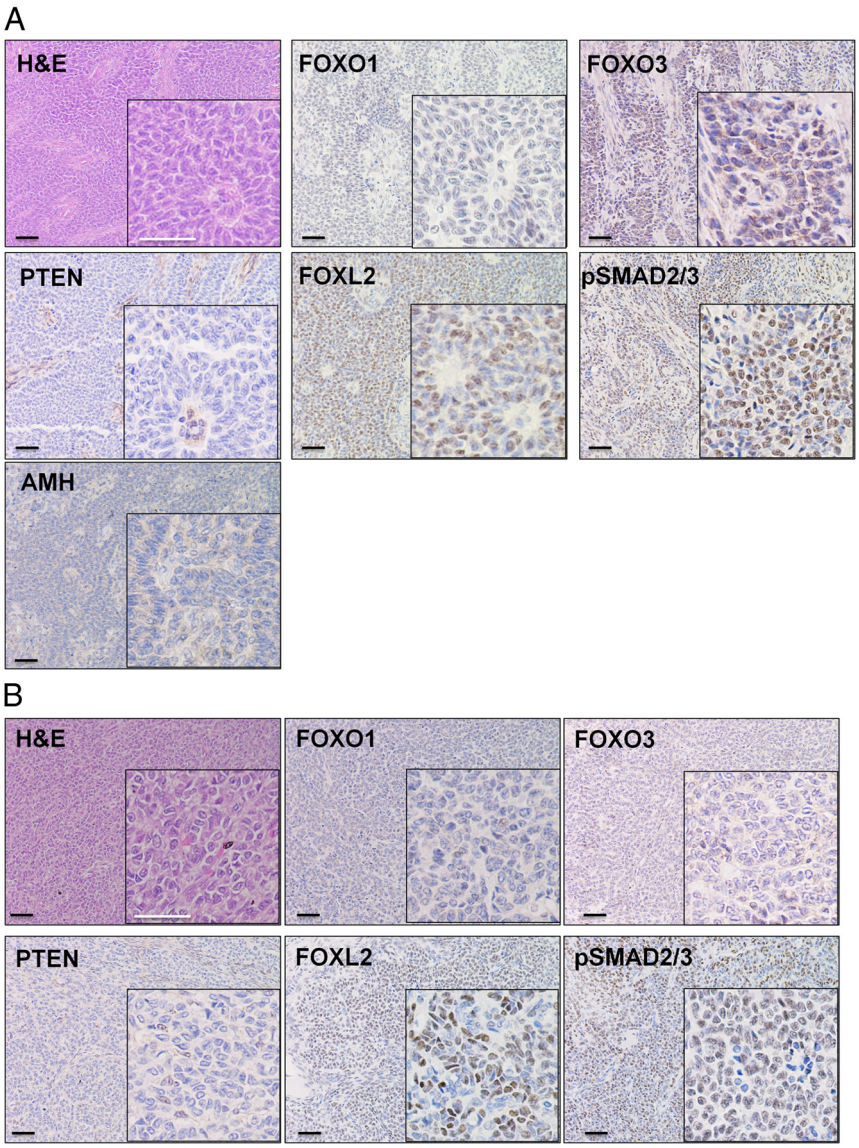

Figure 7. A and B, FOXL2 and pSMAD2/3 are present in hAGCTs. Five hAGCTs samples were sectioned, stained with H&E, or analyzed by IHC for expression of FOXO1, FOXO3, PTEN, FOXL2, pSMAD2/3, and AMH. Two representative samples are shown. In all samples, FOXL2 and pSMAD2/3 were present and nuclear, PTEN was absent, and FOXO1/3 were negligible or cytoplasmic. Scale bars, 200 μm (black) and 80 μm (inset, white).

hAGCTs are FOXL2 and pSMAD2/3 positive

Histological and IHC analyses of hAGCTs showed that the tumors exhibited cords of tumor cells that

contained Call-Exner bodies or appeared more solid (Figure 7, A and B, and Supplemental Figure 2, A and B). In the tumors examined, staining for PTEN was negligible; staining for FOXO1 and FOXO3 was either negligible (Figure 7A) or distinctly cytoplasmic (Figure 7B). Although AMH is variably expressed human juvenile GCTs and hAGCTs) (40, 82), it was not detected in the GCT samples analyzed. However, intense staining for FOXL2 and pSMAD2/3 was observed and similar to that observed in the mouse GCTs.

Gene expression profiles in GCTs from *Foxo1*$^{f/f}$; *Foxo3*$^{f/f}$; *Pten*$^{f/f}$;*Cyp19*-cre

To analyze the gene expression profiles in GCTs of the mutant mice compared with that in control granulosa cells, RNA was prepared from 3 representative GCTs isolated from the ovaries of *Foxo1*$^{f/f}$;*Foxo3*$^{f/f}$; *Pten*$^{f/f}$; *Cyp19*-cre mice at 2–3 months of age. The RNA was pooled and analyzed by microarray Affymetrix platforms. This dataset was then compared with our previous datasets from granulosa cells isolated from immature mice at day 25 of age (GSE35593) (heat map, Supplemental Table 1). Because the vast majority of the cells in the tumors were FOXL2 positive and hence granulosa cell-derived rather than stromal-related this allowed us to compare genes expressed in the GCTs with those expressed in normal granulosa cell populations without the presence of interstitial cells and corpora lutea in adult mouse ovaries. Careful inspection of the microarray alone with Gene Ontology software indicated that many genes associated with granulosa cell differentiation were markedly reduced compared with controls. Genes that are involved in specific signaling cascades known to impact granulosa cell specification, proliferation, gonadal cancer, and differentiation were also dysregulated (Supplemental Table 1).

qPCR analyses on additional RNA samples showed that many granulosa cell-related genes were down-regulated, including *Amh*, *Bmp2*, *Emx2*, *Fshr*, *Fst*, *Lhcgr*, *Nppc*, *Nr0b1*, *Rspo1*, and *Wt1*; others were up-regulated, including *Ccnd1*, *Esr1*, *Grem1*, *Inhbb*, *Krt8*, and *Sox9* (Figure 8 and Supplemental Table 1). Many of the down-regulated genes (*Emx2*, *Rspo1*, *Fst*, and *Wt1*) are known to impact granulosa cell specification and/or follicle formation in the embryonic gonad and some are antitestis genes (24, 83, 84). Thus, it is not surprising that SOX9 was expressed in a subset of tumor cells. Of these

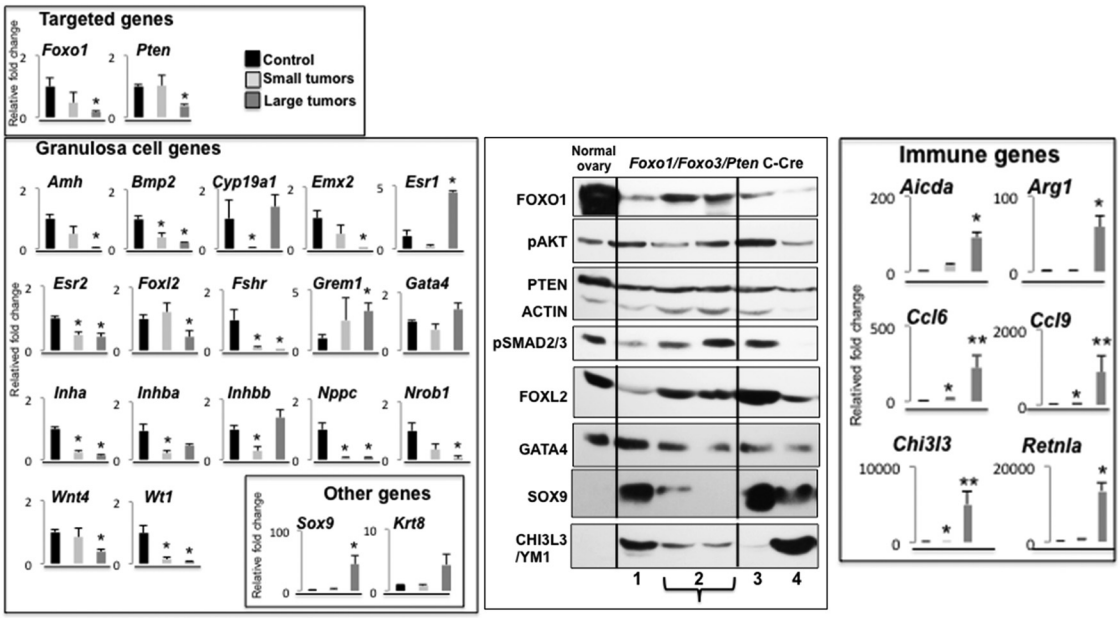

Figure 8. Gene expression profiles in GCTs. To identify global changes in gene expression profiles in the tumors microarray, analyses were done on tumors from the *Foxo1//3/Pten* tKO mice. RNA from tumors of mice shown in Figure 6A, a and b, were pooled and analyzed by mouse Affymetrix platforms. RNA from these and additional tumor samples (n = 9) were used for qPCR analyses to verify the microarray results. In the array and by qPCR, specific granulosa cell genes were show to be down-regulated, including those targeted for disruption, *Foxo1* and *Pten*. Many (*Amh*, *Bmp2*, *Fshr*, *Inha*, *Nppc*, and *Wt1*) were down-regulated in small tumors present at 2–3 months of age; additional genes (*Emx2*, *Inhba*, and *Nrob1*) were down in larger tumors at 3–4 months. *Foxl2* and *Wnt4* mRNA also appeared to decline in the large tumor samples likely due to the greater heterogeneity of the tumors. Genes that were up-regulated significantly included *Sox9*, *Krt8*, and several specific immune-related genes, including *Chi3l3*. Western blot analyses confirmed both the IHC analyses and the qPCR results for several proteins. FOXO1 and PTEN were dramatically lower in the tumors compared with control ovaries from immature mice; FOXL2 was similar to controls in some but not all tumors; SOX9 was absent from the control sample but variably elevated in the tumors. Likewise, the immune related gene CHI3L3 was absent from the control but elevated in the tumors.

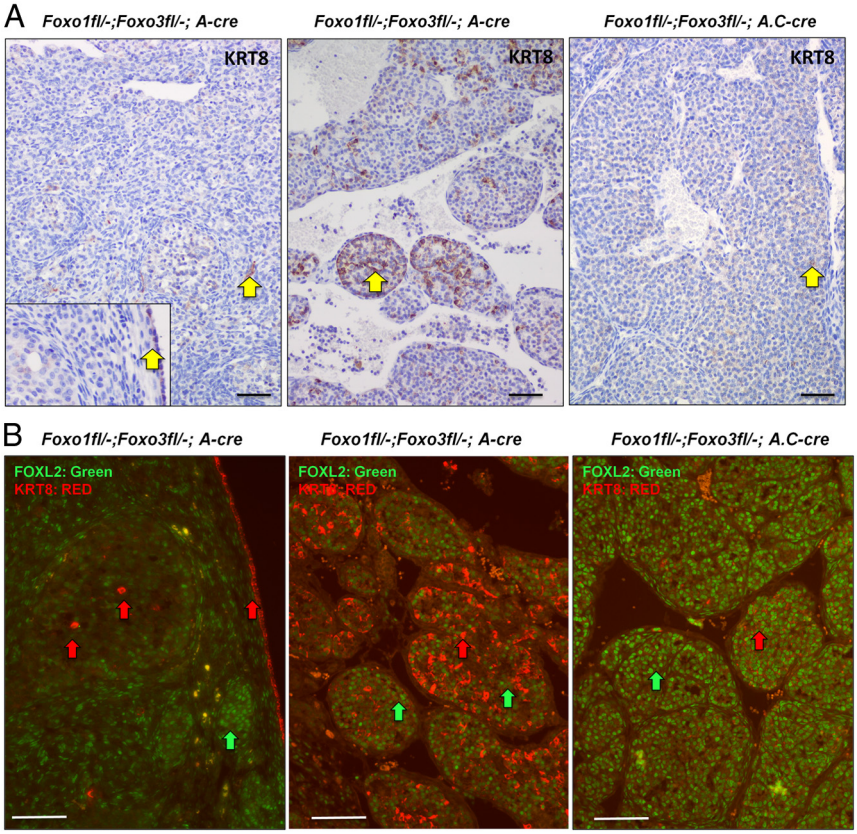

Figure 9. A, KRT8 is expressed in granulosa cells within specific regions of the *Foxo1/3* dKO tumors. Tumors described in Figure 2 were used to examine the immunolocalization of KRT8 in the *Foxo1/3* dKO mice. Positive staining for KRT8 was observed in some granulosa cells within the tumors (left and right panels, yellow arrows) and in the OSE cells (inset, yellow arrow). KRT8 immunostaining was most intense in clusters of cells forming follicle-like structures (middle panel). Scale bars, 40 μm (black). B, Localization of FOXL2 and KRT8 in tumors of the *Foxo1/3* dKO mice. Immunofluorescence analyses were performed to determine whether KRT8 colocalized with FOXL2. As shown, KRT8 staining was present but low in most granulosa cells of the tumors (left and right panels) but was high in the OSE cells (red arrows). KRT8 and FOXL2 staining was intense in the clusters of cells shown in the middle panel, but the cells most intense for KRT8 were not those most intense for FOXL2. Scale bars, 200 μm (white).

down-regulated genes *Nr0b1* is a known target of FOXO1 (61). Importantly, other genes critical for granulosa cell fate and proliferation were not altered markedly in the *Foxo1*$^{f/f}$;*Foxo3*$^{f/f}$; *Pten*$^{f/f}$;*Cyp19*-cre mice. These include *Foxl2* and *Smad3*, as would be predicted from the IHC data but also the transcription factor *Gata4*. GATA4 is not only required for gonadal ridge formation (11) but also for normal follicle development (30) and steroidogenesis (85, 86). GATA4 is also present in hAGCTs (33, 34, 87) and appears to synergize with SMAD3 to promote tumor cell proliferation (33). Thus, GATA4 also appears to be a marker of AGCTs (88).

Western blot analyses confirmed reduced expression of FOXO1 and PTEN in tumors of the *Foxo1/3/Pten* mice compared with ovaries in control mice (Figure 8). In the same samples FOXL2, GATA4, and pSMAD2/3 were present at levels quite similar to that observed in control ovaries. However, FOXL2 was lower in one large tumor that also had higher SOX9 levels. By contrast, SOX9 was absent from control ovaries but was observed in the tumors, especially those that exhibited abundant SOX9 by IHC. Thus, these results document that SOX9 protein is expressed in the tumors. Although PTEN is depleted in the tumor cells, pAKT was not markedly elevated in the granulosa cells of the tumors but was higher in tubular-like structures that are devoid of FOXL2 (Supplemental Figure 3).

The microarrays and qPCR revealed further that mRNAs encoding cytokeratins 7 and 18, in addition to *Krt8*, were elevated in the GCTs (Figure 8). IHC analyses confirmed and documented that many tumor granulosa cells in the *Foxo1/3* dKO and tKO mice were KRT8 positive; cells exhibiting the highest levels of KRT8 were organized in discrete tubular-like structures within the tumors (Figure 9A). These results were intriguing because recent studies have provided provocative evidence that granulosa cells present in the second wave of follicular development in pubertal/adult mice appear to be derived from ovarian surface epithelial (OSE) cells that are known to be KRT8 positive (89–91). Other evidence indicates that pregranulosa cells and pre-OSE cells (that are eventually KRT8 positive) are likely derived from common progenitor cells (92) and in the embryonic gonad express either *Foxl2* or *Lgr5* (93). Given these observations, we sought to determine whether the KRT8 positive cells in the GCTs might also express FOXL2 and/or SOX9 and thereby represent a transition to an epithelial-like cell or Sertoli-like cell. To assess this hypothesis, we costained GCTs of the *Foxo1/3* dKO mice and *Foxo1/3;Pten* tKO mice with KRT8 and either FOXL2 or SOX9 antibodies. Our results indicate that although most *Foxo1/3* GCT cells are FOXL2 positive, only a few also express high levels of KRT8, especially the tumors with tubular-like structures (Figure 9B, green arrows). Immunofluorescent analyses further documented the intense staining of specific cells for KRT8 that did not appear to be positive for FOXL2 (Figure 9B, left and middle panels). However, low levels of KRT8

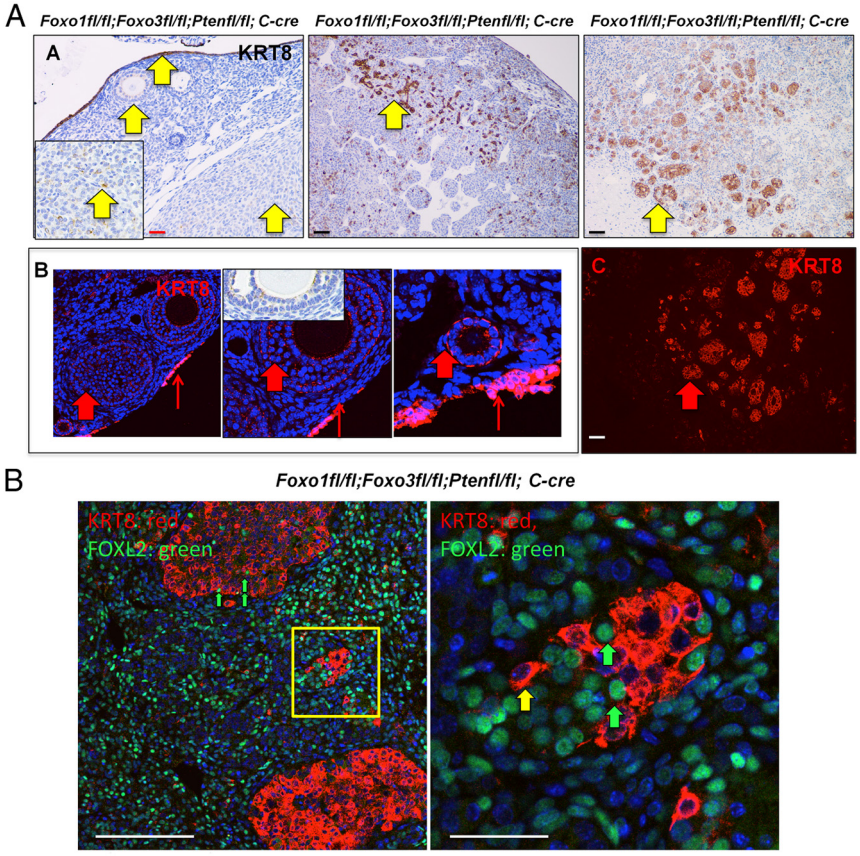

Figure 10. A, KRT8 expression is elevated in large tumors of the *Foxo1/3/Pten* tKO mice. Tumors from the mice shown in Figure 6A were immunostained for KRT8. a, KRT8 staining was high in the ovarian surface epithelium (yellow arrow) surrounding ovarian tissue containing small follicles. Lower levels of KRT8 were present in the granulosa cells of small follicles (yellow arrows) and the cells within the solid tumor (inset, yellow arrows). Many tumor cells and clusters of tumor cells were highly KRT8 positive in the large tumors (middle and right panels, yellow arrows). c, Immunofluorescence confirmed low levels of KRT8 staining in granulosa cells of small follicles (solid red arrows) compared with the ovarian surface epithelium (small red arrow). c, Immunofluorescence also confirmed that KRT8 is highly expressed in specific clusters of cells of this tumor, and therefore, this tumor was further analyzed in Figures 9B and 10). Scale bars, 200 μm (black or white) and 80 μm (red). B, Localization of FOXL2 and KRT8 in tumors of the *Foxo1/3Pten* tKO mice. Dual labeling for FOXL2 (green) and KRT8 (red) in this tumor shows that many cells within the tumor are FOXL2 positive and that select clusters of cells are mostly KRT8 positive with a few FOXL2 positive associated with them. However, FOXL2 does not appear to be colocalized with KRT8 in the same cells (right panel; enlargement of area demarcated in yellow in the left panel). Scale bars, 180 and 41.6 μm, respectively.

were detected in most FOXL2 positive cells in some tumors (Figure 9B, right panel).

Tumors in the *Foxo1/3;Pten* tKO mice, especially those that contained many tubular clusters of cells, also expressed high levels KRT8 (Figure 10Aa, yellow arrows, and c, red arrow). In addition, KRT8 was present at low levels in granulosa cells of small follicles and cells of a solid GCT compared with the elevated levels of KRT8 in the OSE cells (Figure 10Ab, red arrows and inset). As in the tumors of the *Foxo1/3* dKO mutant mice, tumors of the *Foxo1/3* tKO appear to be FOXL2 positive (Figure 10B). However, most FOXL2 cells are not KRT8 positive or express low levels of KRT8. Unexpectedly, many KRT8 positive cells were SOX9 positive (Figure 11). Thus, within the GCTs there are clearly subsets of cells, especially in the *Foxo1/3;Pten* strain, that are positive for KRT8 and FOXL2 or SOX9. Because most tumor cells were positive for pSMAD2/3 it is highly likely that that most KRT8 positive cells also appear to be positive for pSMAD2/3.

The most highly induced genes in the GCTs were those related to autoimmune responses and alternative activation of macrophages (AAMs) as confirmed by qPCR and Western blot analyses (Figure 8) (94). Of particular interest were the elevated levels of the AAM-related genes, *Relna*, *Chi3l3/YM1*, *Arg1*, and *Tgm2*, compared with genes associated with classical inflammation, such as the interleukins and cytokines. qPCR analyses of additional RNA samples confirmed the enhanced expression of *Arg1*, *Chi3l3*, and *Relna* and other immune-related genes in the GCT-bearing ovaries (Figure 7). Moreover, some of the immune-related genes such as *Chi3l3* are slightly elevated in the ovaries of the *Foxo1/3* dKO mice as early as 2 months of age and in the tumors of the *Foxo1/3* dKO mice (Figure 8). Western blot analyses confirmed the elevated expression of CHI3L3 in the tumors but not control ovaries (Figure 8). Notably, these immune cell-related genes are not increased in GCTs present in ovaries of the β-*catenin* (*Ctnnb1*) mutant mice (38) or in OSE tumors that develop in the *Pten/Kras* mutant mice (95), indicating that these AAMs are specific to *Foxo1/3* and *Foxo1/3/Pten* mutant mice.

To determine which cells within the tumors were expressing these immune-related genes, IHC analyses were done. As shown, CHI3L3 positive cells were observed in discrete regions of the GCTs that exhibited tubular-like structures and were KRT8 positive, especially in tumors of *Foxo1/3* dKO mice at 6–8 months of age and *Foxo1/3/Pten* tKO mice at approximately 4 months of age (Figure 12A, yellow arrows). Immunofluorescent analyses further confirmed and documented that many tumors re-

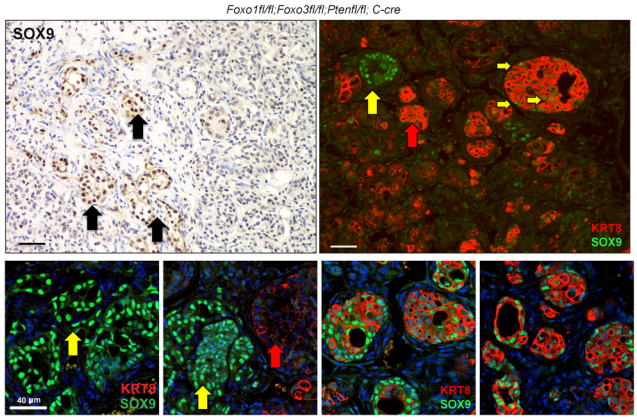

Figure 11. Localization of SOX9 and KRT8 in tumors of the *Foxo1/3Pten* tKO mice. SOX9 positive cells are clearly evident by IHC staining (upper left, black arrows). When tumor cells were dual-labeled for SOX9 and KRT8, several patterns were observed. Some clusters of cells that were only positive for SOX9 (upper right and lower left panels, red arrows), others were only positive for KRT8 (upper panel, lower right, yellow arrows), and some were positive for both (upper right and lower right panels). Scale bar, 40 μm (black) and 40 μm (white).

gions expressing the highest levels of KRT8 were also positive for CHI3L3/YM1 (Figure 12B). However, costaining of KRT8 and CHI3L3/YM1 showed that each protein was localized to discrete cell populations that were in close association, but were not overlapping in these tubular-like structures (Figure 12B). The increased expression of AAM genes and increased numbers of CHI3L3 positive cells appears to be associated with increased infiltration of this specific macrophage subtype because these are not observed in normal ovaries or at early stages of tumor development. However, we cannot rule out differentiation of macrophages within the tumors.

Discussion

These studies document that precise activation and suppression of the PI3K pathway in granulosa cells is essential for normal follicle growth; severe disruption of this pathway impairs follicle development, alters granulosa cell fate decisions, and promotes GCT formation and progression. Specifically, we show that selective depletion of *Foxo1* and *Foxo3* in granulosa cells leads to the development of large GCTs in approximately 20% of the *Foxo1/3* dKO mice and coordinate loss of *Pten* in *Foxo1/3* mutant granulosa cells facilitates early onset and increases the incidence of GCTs to approximately 65% in the *Foxo1/3/Pten* tKO mice. The tumor-promoting synergy between FOXO1/3 and PTEN likely involves: 1) more complete disruption of these genes and components of the PI3K pathway in granulosa cells (59), 2) decreased apoptosis of granulosa cells as a consequence of *Foxo1/3* depletion and reduced expression and activity of BMP2 (61), and/or 3) loss of terminal differentiation and cell cycle exit that normally occurs with follicular development and ultimately the transition of granulosa cells to nondividing luteal cells (96, 97).

Specifically, our results indicate that increased levels of activin (INHβB) and elevated phosphorylation/activation of SMAD2/3, in the absence of FOXO1/3 and PTEN, serve to prevent differentiation and promote granulosa cell proliferation and tumor formation. The lack of tumor cell differentiation is likely enhanced by the high levels of inhibin and other factors that inhibit pituitary expression of *Fshb* and *Lhb* mRNAs, leading to severely reduced levels of serum FSH and LH. These results are of clinical relevance, because serum FSH is also markedly reduced and INHβB is elevated in patients with AGCTs (98). However, the ability of exogenous gonadotropins to enhance early onset and growth of GCT formation in the *Foxo1/3* and *Foxo1/3/Pten* mutant mice indicates that brief exposure to gonadotropins, rather than long-term exposure (99), likely contributes to GCT formation and growth in this context. Thus, the onset of the adult-type GCTs in perimenopausal women indicates that elevated gonadotropins and altered functions of the PI3K pathway likely facilitate the initiation of GCT proliferation but are not required to maintain tumor growth in the presence of elevated INHβB.

The GCTs in the *Foxo1/3* and *Foxo1/3/Pten* mutant mice exhibit striking and specific alterations in gene expression profiles compared with granulosa cells of control mice. Specifically, the tumor cells retain expression of FOXL2, GATA4, and WNT4, markers of pregranulosa cells and granulosa cells in small follicles. The tumor cells also retain expression of factors that regulate FOXL2 activity, such as *Lats1/2* (100–102; data not shown). However, they lack expression of other key genes that control granulosa cell fate specification and follicle formation (*Emx2*, *Fst*, *Lgr5*, *Nr0b1*, and *Rspo1*) and differentiation (*Amh*, *Fshr*, and *Lhcgr*) (23, 24, 83, 103–109). The loss of *Rspo1* likely contributes to the decreased expression of *Emx2* and *Amh* because both are regulated by WNT4 signaling in granulosa cells (24). Furthermore, *Emx2* knockout mice lack gonads (and kidneys) (110) that is associated with severely abnormal embryonic gonadal ridge development (83). In addition to its role in reproductive and neural development (111), *Emx2* appears to impact tumorigenesis (112). Thus, the absence of *Emx2* in the GCTs likely promotes proliferation. Reduced levels of *Amh*, a negative regulator of granulosa cell proliferation, combined with low levels of *Bmp2* and increased *Grem1* that inhibits BMP activity promote apoptosis, and reduced levels of *Fst* and *Tgfb3* (betaglycan)

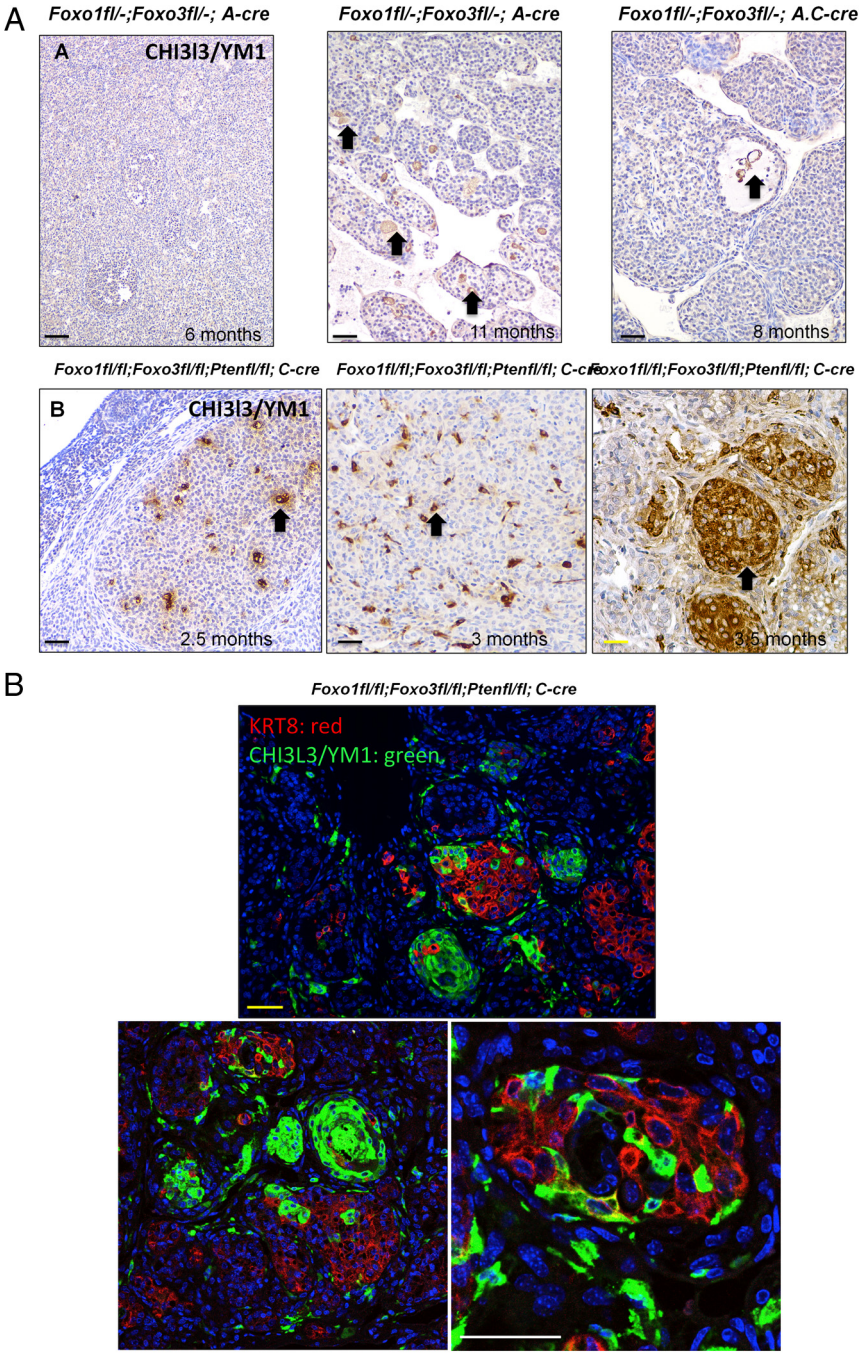

Figure 12. A, Localization of CHI3L3 in tumors of the *Foxo1/3* dKO and *Foxo1/3Pten* tKO mice. CHI3L3 (also known as YM1) was localized to specific cells in tumors of both the (a) *Foxo1/3* dKO mice (shown in Figure 2) and (b) *Foxo1/3Pten* tKO mice (shown in Figure 6A, black arrows). However, there were many more CHI3L3 positive cells in tumors of the *Foxo1/3Pten* tKO mice (b), where they appeared as single cells or were present in clusters of cells (black arrows). Scale bars, 100 μm (black) and 50 μm (white). B, Localization of CHI3L3 positive cells and KRT8 positive cells. Immunofluorescence analyses show that CHI3L3 positive cells (green) and KRT8 positive cells (red) are found within the same clusters of cells but are not or rarely colocalized within the same cells. Scale bar, 50 μm (yellow) and 60 μm (white).

that antagonize activin signaling may also collectively contribute to tumor cell proliferation (104, 113–115) even in the presence of inhibin in the *Foxo1/3/Pten* mutant context. Reduced levels of *Amh* may also be related to the activity of FOXL2 (18). These altered gene expression profiles are consistent with abnormal follicle development and the dramatic loss of oocytes that is also observed in ovaries of the *Emx2*, *Rspo1*, and *Wnt4* knockout mice (24, 107, 108). In addition, in the embryonic ovary activin can cause apoptosis of germ cells (116). Therefore, at the ovarian level elevated amounts of activin (INHβB), in the absence of BMP2 and FOXO1/3, may mediate marked changes in granulosa cells that lead to the early loss of oocytes that occurs in these mutant mice.

Our results indicate further that the GCTs in the *Foxo1/3* and *Foxo1/3Pten* mutant mice exhibit features similar to hAGCTs and KGN cells (6, 8, 33) rather than to the juvenile GCTs and COV434 cells (6, 40). Of particular relevance, the expression profiles for many of genes are similarly altered in the *Foxo1/3/Pten* GCTs, AGCTs, and KGN cells compared with the COV434 cells: *AMH*, *FOXO1*, and *EMX2* are down-regulated; *FOXL2*, *GATA4*, *SMAD3*, *INHBB*, and *SOX9* are present (17, 18, 33). Furthermore, the intense immunostaining and colocalization of FOXL2 and pSMAD2/3 in nuclei of cells within the AGCTs combined with the lack of PTEN and low/cytoplasmic localization of FOXO1 was similar to that in the GCTs of the *Foxo1/3* and *Foxo1/3Pten* mutant mice. In addition, recent microarray analyses of AGCTs provides evidence that FOXL2 regulates expression of both cytochrome p450, family 19, subfamily A, polypeptide 1 and estrogen receptor 2 contributing to estrogen signaling in AGCTs (28).

Remarkably, the dramatic loss of *Emx2*, *Kitl*, *Nr0b1*, and *Rspo1* in the *Foxo1/3/Pten* GCTs does not lead to global reversal to a testicular phenotype as occurs in the *Wnt4* and *Rspo1* KO mice or in humans lacking *RSPO1* (117). The lack of gonadal sex reversal in these mice may be explained, in

part, by 1) the presence of *Wnt4*; 2) the potent effects of FOXL2, GATA4, and activin in promoting granulosa cell fate specification and GCT growth (33); and 3) the lack of expression of genes required for complete transdifferentiation of granulosa cells to Sertoli cells (22). Specifically, it is well established that the Sertoli cell marker SOX9 is low or absent from granulosa cells of growing follicles in wild-type mice and human ovaries (77–79) and that depletion of FOXL2, especially when combined with the depletion of WNT4, leads to increased expression of SOX9 and other genes required for an ovary to testis phenotypic transition (109). Of note, we see a transition state in a subset of follicle-like structures where some granulosa cells exhibit low levels of both FOXL2 and SOX9 and other cells exhibit specific expression of SOX9 and the exclusion of FOXL2. However, we do not yet know the mechanisms that control this switch in only a select subgroup of the *Foxo1/3* mutant cells and follicles. That other Sertoli-cell genes, such as *Rhox8*, *Sox8*, and *Tsx*, are not increased in the GCTs indicates that SOX9 alone is not sufficient, in this context, to drive the transdifferentiation of granulosa cells to Sertoli cells in the *Foxo1/3/Pten* mutant mouse ovaries. In this regard, it is important to note that the human granulosa tumor KGN cell line that has been derived from an AGCT expresses low or negligible levels of FOXO1 and increased levels of SOX9 compared with COV434 cells that were derived from a human juvenile GCT (18). Although previous studies ruled out mutation and amplification of AKT/PI3K pathway components in KGN cells as the basis for GCT formation (118), the expression and activity of PTEN and other downstream targets (tuberous sclerosis 1 and raptor) that recently have been shown to impact follicle activation, including FOXO1, were not analyzed (118). Our results extend these observations and show for the first time that inactivation and/or loss of FOXO1/3 and PTEN promotes expression of FOXL2, GATA4, and chronic phosphorylation of SMAD2/3, and this combined with low expression of other factors leads to altered granulosa cell proliferation and fate decisions. Similar events appear to occur in adult-type GCTs in women (data here and Figure 8, A and B) (33), but the precise mechanisms remain to be determined.

Additionally, many granulosa cells in the GCTs of the *Foxo1/3* and *Foxo1/3/Pten* mutant mice express detectible or even elevated levels of KRT8, a marker of epithelial cells and the organization of the GCTs into tubular-, epithelial-like structures. These observations indicate that granulosa cells lacking *Foxo1/3/Pten* may be 1) reverting to a phenotype characteristic of progenitor granulosa-epithelial cells found in the embryonic gonad (92) or 2) transitioning to an epithelial-like phenotype typical of OSE cells, from which they may also be derived (89, 119). Quite strikingly, some but not all of the KRT8+ cells express SOX9. Importantly, SOX9 is expressed in epithelial cells of the endometrium and Fallopian tube and in epithelia ovarian cancer (77, 78), indicating that it is a marker of these cells as well as Sertoli cells. That *Sox9*, *Krt8*, and *Krt18* are elevated in KGN cells provides further evidence that AGCTs in women may also exhibit epithelial like characteristics. However, we did not detect KRT8 in the hAGCTs analyzed here. Thus, SOX9 expression in the mouse GCTs may be more a reflection of a transition to an epithelial like phenotype rather than to a Sertoli-like cell.

Our results have also documented that many of the *Foxo1/3/Pten* GCTs are associated with a pronounced and specific immune response that is not observed in GCTs that develop in the *Ctnnb;Pten*, *Ctnnb1;Kras*, or *Smad1/5* mutant mice (10, 38, 40). Moreover, the immune response exhibits characteristics of AAMs as indicated by the expression of specific genes, including *Retnla*, *Arg1*, *Tgm2*, and *Chi3l3* (94, 120, 121). These genes are distinct from those associated with the classic activation of macrophages that leads to increased production of inflammatory factors, including ILs,

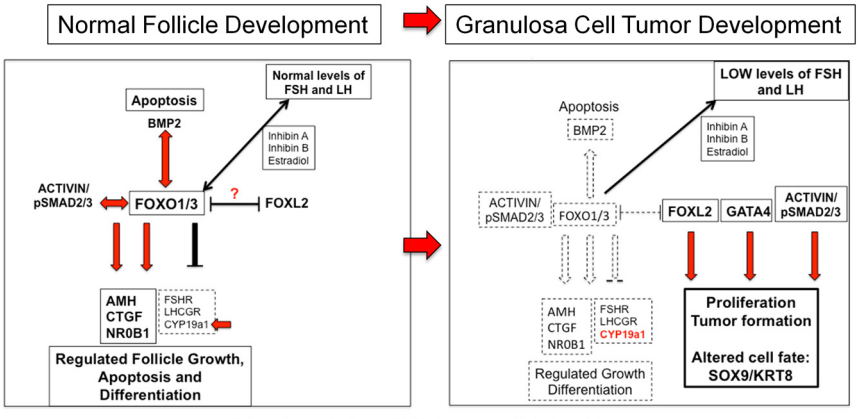

(From Liu *et al*, 2013; Data presented herein)

Figure 13. FOXO1/3 and PTEN depletion alters granulosa cell fate decisions, leading to proliferation and tumor formation. FOXO1 and FOXO3 along with PTEN are gatekeepers of follicle development by regulating granulosa cell functions. FOXO1/3 interact with activin and pSMAD2/3 to regulate genes involved in follicle growth and represses genes (*Fshr*, *Lhcgr*, and *Cyp19a1*) associated with differentiation. With BMP2, FOXO1/3 act to regulate apoptosis and genes controlling the apoptotic pathway. FOXO1, FOXO3, and FOXL2 are expressed in the same cells of growing follicles. Thus, it is possible that they interact to control each other's functions. Once FOXO1/3 and PTEN are inactivated, FOXL2, GATA4, and pSMAD2/3 promote unopposed proliferation and lead to changes in cell fate decisions.

prostaglandin synthase 2, and pentraxin 3. Although AAMs are most frequently associated with allergic responses, they are also associated with cancer and are a marker of poor prognosis (121). The expression of CHI3L3 in specific macrophages present in the large GCTs indicates that they are regulating specific events that may include angiogenesis. CHI3L3 can bind to the interleukin 13 receptor a2 to mediate specific regulatory effects (120).

In summary, FOXO1, FOXO3, and PTEN coordinately exert potent regulatory effects in granulosa cells of growing follicles that promote and sustain normal follicle growth and prevent unrestricted granulosa cell proliferation and GCT formation (Figure 13). The unrestricted tumor cell proliferation is associated with the expression of FOXL2, GATA4, and activinβB and sustained phosphorylation and nuclear localization of SMAD2/3. It is also associated with *Esr2*, increased *Esr1*, and *Ccnd1*. That these same factors are present and characterize adult-type GCTs in women (data here and Refs. 28, 33) provides strong evidence that that altered signaling in the PTEN/PI3K/FOXO and activin pathways are associated with a subset of GCTs in women (33). Activin signaling may be chronically activated in the GCTs because 1) FOXO1 can no longer induce expression and interact with BMP2 signaling to promote apoptosis (61); 2) the BMP inhibitor gremlin 1 is elevated and may act to further suppress the BMP/SMAD1/5 signaling (97); 3) expression of *Amh* is negligible and thus the growth inhibitory effects of AMH are lost (104); 4) expression of *Fshr* and levels of serum FSH are negligible, preventing signaling through the cAMP pathway that supports differentiation (97, 105, 122); and 5) other tumor suppressor genes, such as *Emx2* (112), are markedly reduced. Thus, although FOXO3 and PTEN act in oocytes to maintain quiescence of primordial follicles (63, 81, 122), FOXO1, FOXO3, and PTEN act as the gatekeepers of follicle development by controlling granulosa cell proliferation, apoptosis and differentiation (Figure 13). These features indicate that the *Foxo1/3/Pten* mutant mice provide a good in vivo model that recapitulates many features of adult-type GCTs in women and, thereby, strong evidence that impaired functions of the PTEN/PI3K/FOXO pathway lead to dramatic changes in the molecular program within granulosa cells, chronic phosphorylation of SMAD2/3 in the presence of FOXL2 and GATA4, and tumor formation.

Acknowledgments

Address all correspondence and requests for reprints to: JoAnne S. Richards, PhD, Department of Molecular and Cellular Biology, One Baylor Plaza, Houston, TX 77030. E-mail: joanner@bcm.edu.

Ligand Assay and Analysis Core is supported by the *Eunice Kennedy Shriver* National Institute of Child Health and Human Development/National Institutes of Health through cooperative agreement (U54-HD28934) as part of the Specialized Cooperative Centers Program in Reproduction and Infertility Research.

Disclosure Summary: The authors have nothing to disclose.

References

1. **Bast RC Jr, Hennessy B, Mills GB.** The biology of ovarian cancer: new opportunities for translation. *Nat Rev Cancer*. 2009;9:415–428.
2. **Romero I, Bast RC Jr.** Minireview: human ovarian cancer: biology, current management, and paths to personalizing therapy. *Endocrinology*. 2012;153:1593–1602.
3. **Karst AM, Drapkin R.** Ovarian cancer pathogenesis: a model in evolution. *J Oncol*. 2010; 2010:932371.
4. **Lengyel E.** Ovarian cancer development and metastasis. *Am J Path*. 2010;177:1053–1064.
5. **Mullany LK, Richards JS.** Minireview: animal models and mechanisms of ovarian cancer development. *Endocrinology*. 2012;153:1585–1592.
6. **Jamieson S, Fuller PJ.** Molecular pathogenesis of granulosa cell tumors of the ovary. *Endocr Rev*. 2012;33:109–144.
7. **Jubb I, Kennedy KVF, Palmer N.** *Pathology of Domestic Animals*. 4th ed. San Diego, CA: American Press; 1993.
8. **Schumer ST, Cannistra SA.** Granulosa cell tumor of the ovary. *J Clin Oncol*. 2003;21:1180–1189.
9. **Dilworth JP.** Non-germ cell tumors of testis. *Urology*. 1991;37:399–417.
10. **Richards JS, Fan HY, Liu Z, et al.** Either Kras activation or Pten loss similarly enhances the dominant-stable CTNNB1-induced genetic program to promote granulosa cell tumor development in the ovary and testis. *Oncogene*. 2012;31:1504–1520.
11. **Hu Y-C, Okumura LM, Page DC.** Gata4 is required for formation of the genital ridge in mice. *PLoS Genet*. 2013;9:e1003629.
12. **Shah SP, Köbel M, Senz J, et al.** Mutation of FOXL2 in granulosa-cell tumors for the ovary. *N Engl J Med*. 2009;360:2719–2729.
13. **Köbel M, Gilks CB, Huntsman DG.** Adult-type granulosa cell tumors and FOXL2 mutation. *Cancer Res*. 2009;69:9160–9162.
14. **Jamieson S, Butzow R, Andersson N, et al.** The FOXL2 C134W mutation is characteristic of adult granulosa cell tumors of the ovary. *Mod Pathol*. 2010;23:1477–1485.
15. **Kalfa N, Philibert P, Patte C, et al.** Extinction of FOXL2 expression in aggressive ovarian granulosa cell tumors in children. *Fertil Steril*. 2007;87:896–901.
16. **Kim JH, Yoon S, Park M, et al.** Differential apoptotic activities of wild-type FOXL2 and the adult-type granulosa cell tumor-associated mutant FOXL2 (C134W). *Oncogene*. 2011;30:1653–1663.
17. **Rosario R, Araki H, Print CG, Shelling AN.** The transcriptional targets of mutant FOXL2 in granulosa cell tumours. *PLoS One*. 2012;7:e46270.
18. **Batista F, Vaiman D, Dausset J, Fellous M, Veitia RA.** Potential targets of FOXL2, a transcription factor involved in craniofacial and follicular development, identified by transcriptomics. *Proc Natl Acad Sci USA*. 2007;104:3330–3335.
19. **Moumné L, Batista F, Benayoun BA, et al.** The mutations and potential targets of the forkhead transcription factor FOXL2. *Mol Cell Endocrinol*. 2008;282:2–11.
20. **Fleming NI, Knower KC, Lazarus KA, Fuller PJ, Simpson ER, Clyne CD.** Aromatase is a direct target of FOXL2:C134W in granulosa

cell tumors via a single highly conserved binding site in the ovarian specific promoter. *PLoS One*. 2010;5:e14389.
21. **Rosario R, Wilson M, Cheng WT, et al.** Adult granulosa cell tumours (GCT): clinicopathological outcomes including FOXL2 mutational status and expression. *Gynecol Oncol*. 2013;131:325–329.
22. **Uhlenhaut NH, Jakob S, Anlag K, et al.** Somatic sex reprogramming of adult ovaries to testes by FOXL2 ablation. *Cell*. 2009;139:1130–1142.
23. **Uda M, Ottolenghi C, Crisponi L, et al.** Foxl2 disruption causes mouse ovarian failure by pervasive blockage of follicle development. *Hum Mol Genet*. 2004;13:1171–1181.
24. **Garcia-Ortiz JE, Pelosi E, Omari S, et al.** Foxl2 functions in sex determination and histogenesis throughout mouse ovary development. *BMC Dev Biol*. 2009;9:36.
25. **Schmidt D, Ovitt CE, Anlag K, et al.** The murine winged-helix transcription factor Foxl2 is required for granulosa cell differentiation and ovary maintenance. *Development*. 2004;131:933–942.
26. **Caburet S, Georges A, L'Hôte D, Todeschini AL, Benayoun BA, Veitia RA.** The transcription factor FOXL2: at the crossroads of ovarian physiology and pathology. *Mol Cell Endocrinol*. 2012;356:55–64.
27. **Georges A, Auguste A, Bessière L, Vanet A, Todeschini AL, Veitia RA.** FOXL2: a central transcription factor of the ovary. *J Mol Endocrinol*. 2014;52:R17–R33.
28. **Georges A, Hôte D, Todeschini AL, et al.** The transcription factor FOXL2 mobilizes estrogen signaling to maintain the identity of ovarian granulosa cells. *eLife*. 2014;3.
29. **Padua MB, Fox SC, Jiang T, Morse DA, Tevosian SG.** Simultaneous gene deletion of Gata4 and Gata6 leads to early disruption of follicular development and germ cell loss in the murine ovary. *Biol Reprod*. 2014;91:24.
30. **Bennett J, Wu YG, Gossen J, Zhou P, Stocco C.** Loss of GATA-6 and GATA-4 in granulosa cells blocks folliculogenesis, ovulation, and follicle stimulating hormone receptor expression leading to female infertility. *Endocrinology*. 2012;153:2474–2485.
31. **Matzuk MM, Finegold MJ, Su JG, Hsueh AJ, Bradley A.** α-Inhibin is a tumour-suppressor gene with gonadal specificity in mice. *Nature*. 1992;360:313–319.
32. **Tao X, Sood AK, Deavers MT, et al.** Anti-angiogenesis therapy with bevacizumab for patients with ovarian granulosa cell tumors. *Gynecol Oncol*. 2009;114:431–436.
33. **Anttonen M, Pihlajoki M, Andersson N, et al.** FOXL2, GATA4, and SMAD3 co-operatively modulate gene expression, cell viability and apoptosis in ovarian granulosa cell tumor cells. *PLoS One*. 2014;9:e85545.
34. **Benayoun BA, Anttonen M, L'Hôte D, et al.** Adult ovarian granulosa cell tumor transcriptomics: prevalence of FOXL2 target genes misregulation gives insights into the pathogenic mechanism of the p.Cys134Trp somatic mutation. *Oncogene*. 2013;32:2739–2746.
35. **Pangas SA, Li X, Umans L, et al.** Conditional deletion of Smad1 and Smad5 in somatic cells of male and female gonads leads to metastatic tumor development in mice. *Mol Cell Biol*. 2008;28:248–257.
36. **Edson MA, Nalam RL, Clementi C, et al.** Granulosa cell-expresed BMPR1A and BMPR1B have unique functions in regulating fertility but act redundantly to suppress ovarian tumor development. *Mol Endocrinol*. 2010;24:1251–1266.
37. **Laguë MN, Paquet M, Fan HY, et al.** Synergistic effects of Pten loss and WNT/CTNNB1 signaling pathway activation in ovarian granulosa cell tumor development and progression. *Carcinogenesis*. 2008;29:2062–2072.
38. **Boerboom D, White LD, Dalle S, Courty J, Richards JS.** Dominant-stable β-catenin expression causes cell fate alterations and Wnt signaling antagonist expression in a murine granulosa cell model. *Cancer Res*. 2006;66:1964–1973.
39. **Mansouri-Attia N, Tripurani SK, Gokul N, et al.** TGFβ signaling promotes juvenile granulosa cell tumorigenesis by suppressing apoptosis. *Mol Endocrinol*. 2014;28:1887–1898.
40. **Middlebrook BS, Eldin K, Li X, Shivasankaran S, Pangas SA.** Smad1-Smad5 ovarian conditional knockout mice develop a disease profile similar to the juvenile form of human granulosa cell tumors. *Endocrinology*. 2009;150:5208–5217.
41. **Rao MC, Midgley AR Jr, Richards JS.** Hormonal regulation of ovarian cellular proliferation. *Cell*. 1978;14:71–78.
42. **Zhou J, Kumar TR, Matzuk MM, Bondy C.** Insulin-like growth factor I regulates gonadotropin responsiveness in the murine ovary. *Mol Endocrinol*. 1997;11:1924–1933.
43. **Arraztoa JA, Kadadia R, Bondy C, Zhou J.** Impaired granulosa cell proliferation in the *IGF1* null ovary. The 83rd Annual Meeting of The Endocrine Society, Denver, CO, 2001 (Abstract P2–393, PP 377).
44. **Zhou P, Baumgarten SC, Wu Y, et al.** IGF-I signaling is essential for FSH stimulation of AKT and steroidogenic genes in granulosa cells. *Mol Endocrinol*. 2013;27:511–523.
45. **Gonzalez-Robayna IJ, Falender AE, Ochsner S, Firestone GL, Richards JS.** FSH stimulates phosphorylation and activation of protein kinase B (PKB/Akt) and serum and glucocorticoid-induced kinase (Sgk): evidence for A kinase independent signaling in granulosa cells. *Mol Endocrinol*. 2000;14:1283–1300.
46. **Baumgarten SC, Convissar SM, Fierro MA, Winston NJ, Scoccia B, Stocco C.** IGF1R signaling is necessary for FSH-induced activation of AKT and differentiation of human cumulus granulosa cells. *J Clin Endocrinol Metab*. 2014;99:2995–3004.
47. **Wayne CM, Fan HY, Cheng X, Richards JS.** Follicle-stimulating hormone induces multiple signaling cascades: evidence that activation of Rous sarcoma oncogene, RAS, and the epidermal growth factor receptor are critical for granulosa cell differentiation. *Mol Endocrinol*. 2007;21:1940–1957.
48. **Rico C, Laguë MN, Lefèvre P, et al.** Pharmacological targeting of mammalian target of rapamycin inhibits ovarian granulosa cell tumor growth. *Carcinogenesis*. 2012;33:2283–2292.
49. **Higgins PA, Brady A, Dobbs SP, Salto-Tellez M, Maxwell P, McCluggage WG.** Epidermal growth factor receptor (EGFR), HER2 and insulin-like growth factor-1 receptor (IGF-1R) status in ovarian adult granulosa cell tumours. *Histopathology*. 2014;64:633–638.
50. **Andersson N, Anttonen M, Färkkilä A, et al.** Sensitivity of human granulosa cell tumor cells to epidermal growth factor receptor inhibition. *J Mol Endocrinol*. 2014;52:223–234.
51. **Brunet A, Bonni A, Zigmond MJ, et al.** Akt promotes cell survival by phosphorylating and inhibiting a forkhead transcription factor. *Cell*. 1999;96:857–868.
52. **Accili D, Arden KC.** FoxOs at the crossroads of cellular metabolism, differentiation, and transformation. *Cell*. 2004;117:421–426.
53. **Kenyon C.** A pathway that links reproductive status to lifespan in *Caenorhabditis elegans*. *Ann NY Acad Sci*. 2010;1204:156–162.
54. **Richards JS, Sharma SC, Falender AE, Lo YH.** Expression of FKHR, FKHRL1, and AFX genes in the rodent ovary: evidence for regulation by IGF-I, estrogen, and the gonadotropins. *Mol Endocrinol*. 2002;16:580–599.
55. **Hosaka T, Biggs WH 3rd, Tieu D, et al.** Disruption of forkhead transcription factor (FOXO) family members in mice reveals their functional diversification. *Proc Natl Acad Sci USA*. 2004;101:2975–2980.
56. **Arden KC.** FoxOs in tumor suppression and stem cell maintenance. *Cell*. 2007;128:235–237.
57. **Tothova Z, Kollipara R, Huntly BJ, et al.** FoxOs are critical mediators of hematopoietic stem cell resistance to physiologic oxidative stress. *Cell*. 2007;128:325–339.
58. **Paik JH, Kollipara R, Chu G, et al.** FoxOs are lineage-restricted redundant tumor suppressors and regulate endothelial cell homeostasis. *Cell*. 2007;128:309–323.
59. **Fan HY, Liu Z, Cahill N, Richards JS.** Targeted disruption of *Pten*

in ovarian granulosa cells enhances ovulation and extends the life span of luteal cells. *Mol Endocrinol*. 2008;22:2128–2140.
60. **Pisarska MD, Kuo FT, Tang D, Zarrini P, Khan S, Ketefian A.** Expression of forkhead transcription factors in human granulosa cells. *Fertil Steril*. 2009;91:1392–1394.
61. **Liu Z, Castrillon DH, Zhou W, Richards JS.** FOXO1/3 depletion in granulosa cells alters follicle growth, death and regulation of pituitary FSH. *Mol Endocrinol*. 2013;27:238–252.
62. **Liu Z, Rudd MD, Hernandez-Gonzalez I, et al.** FSH and FOXO1 regulate genes in the sterol/steroid and lipid biosynthetic pathways in granulosa cells. *Mol Endocrinol*. 2009;23:649–661.
63. **Castrillon DH, Miao L, Kollipara R, Horner JW, DePinho RA.** Suppression of ovarian follicle activation in mice by the transcription factor Foxo3a. *Science*. 2003;301:215–218.
64. **Tarnawa ED, Baker MD, Aloisio GM, Carr BR, Castrillon DH.** Gonadal expression of Foxo1, but not Foxo3, is conserved in diverse mammalian species. *Biol Reprod*. 2013;88:103.
65. **Hsueh AJ, Kawamura K, Cheng Y, Fauser BC.** Intraovarian control of early folliculogenesis. *Endocr Rev*. 2015;36:1–24.
66. **Kawamura K, Cheng Y, Suzuki N, et al.** Hippo signaling disruption and Akt stimulation of ovarian follicles for infertility treatment. *Proc Natl Acad Sci USA*. 2013;110:17474–17479.
67. **Boerboom D, Paquet M, Hsieh M, et al.** Misregulated Wnt/β-catenin signaling leads to ovarian granulosa cell tumor development. *Cancer Res*. 2005;65:9206–9215.
68. **Lesche R, Groszer M, Gao J, et al.** Cre/loxP-mediated inactivation of the murine Pten tumor suppressor gene. *Genesis*. 2002;32:148–149.
69. **Polanco JC, Wilhelm D, Davidson TL, Knight D, Koopman P.** Sox10 gain-of-function causes XX sex reversal in mice: implications for human 22q-linked disorders of sex development. *Hum Mol Genet*. 2010;19:506–516.
70. **Irizarry RA, Hobbs B, Collin F, et al.** Exploration, normalization, and summaries of high density oligonucleotide array probe level data. *Biostatistics*. 2003;4:249–264.
71. **Gentleman RC, Carey VJ, Bates DM, et al.** Bioconductor: open software development for computational biology and bioinformatics. *Genome Biol*. 2004;5:R80.
72. **Rozen S, Skaletsky H.** Primer3 on the WWW for general users and for biologist programmers. *Methods Mol Biol*. 2000;132:365–386.
73. **Kanthan R, Senger J-L, Kanthan S.** The multifaceted granulosa cell tumours-myths and realities: a review. *ISRN Obstet Gynecol*. 2012;2012:878635.
74. **Call EL, Exner S.** Zur Kenntniss des Graafschen Follikels und des Corpus luteum beim Kaninchen. Mathematish naturwssenschaftliche Classe 1875;72:321–328.
75. **Ali S, Gattuso P, Howard A, Mosunjac MB, Siddiqui MT.** Adult granulosa cell tumor of the ovary: fine-needle-aspiration cytology of 10 cases and review of literature. *Diagn Cytopathol*. 2008;36:297–302.
76. **Young RH, Scully RE.** Endocrine tumors of the ovary. *Curr Top Pathol*. 1992;85:113–164.
77. **Uhlen M, Oksvold P, Fagerberg L, et al.** Towards a knowledge-based Human Protein Atlas. *Nat Biotech*. 2010;28:1248–1250.
78. **Uhlen M.** *The Human Protein Atlas*. 2014; version 13. Available at http://www.proteinatlas.org/. Accessed June 18, 2015.
79. **Munger SC, Capel B.** Sex and the circuitry: progress toward a systems-level understanding of vertebrate sex determination. *Wiley Interdiscip Rev Syst Biol Med*. 2012;4:401–412.
80. **Lan ZJ, Xu X, Cooney AJ.** Differential oocyte-specific expression of Cre recombinase activity in GDF-9-iCre, Zp3cre, and Msx2Cre transgenic mice. *Biol Reprod*. 2004;71:1469–1474.
81. **Reddy P, Liu L, Adhikari D, et al.** Oocyte-specific deletion of Pten causes premature activation of the primordial follicle pool. *Science*. 2008;319:611–613.
82. **Färkkilä A, Koskela S, Bryk S, et al.** The clinical utility of serum anti-Müllerian hormone in the follow-up of ovarian adult-type granulosa cell tumors-A comparative study with inhibin B [published online March 24, 2015]. *Int J Cancer*. doi:10.1002/ijc.29532.
83. **Kusaka M, Katoh-Fukui Y, Ogawa H, et al.** Abnormal epithelial cell polarity and ectopic epidermal growth factor receptor (EGFR) expression induced in Emx2 KO embryonic gonads. *Endocrinology*. 2010;151:5893–5904.
84. **Herrera L, Ottolenghi C, Garcia-Ortiz JE, et al.** Mouse ovary developmental RNA and protein markers from gene expression profiling. *Dev Biol*. 2005;279:271–290.
85. **Silverman E, Yivgi-Ohana N, Sher N, Bell M, Elmerl S, Orly J.** Transcriptional activation of sterodogenic acute regulatory protein (StAR) gene: GATA4 and CCAAT/enhancer binding protein β confer synergistic responsiveness in hormone-treated rat granulosa cells and HEK293 cell models. *Endocrinology*. 2006;252:92–101.
86. **Stocco C.** Aromatase expression in the ovary: hormonal and molecular regulation. *Steroids*. 2008;73:473–487.
87. **Anttonen M, Unkila-Kallio L, Leminen A, Butzow R, Heikinheimo M.** High GATA-4 expression associates with aggressive behavior, whereas low anti-Müllerian hormone expression associates with growth potential of ovarian granulosa cell tumors. *J Clin Endocrinol Metab*. 2005;90:6529–6535.
88. **Färkkilä A, Andersson N, Bützow R, et al.** HER2 and GATA4 are new prognostic factors for early-stage ovarian granulosa cell tumor-a long-term follow-up study. *Cancer Med*. 2014;3:526–536.
89. **Mork L, Maatouk DM, McMahon JA, et al.** Temporal differences in granulosa cell specification in the ovary reflect distinct follicle fates in mice. *Biol Reprod*. 2012;86:37.
90. **Zheng W, Zhang H, Liu K.** The two classes of primordial follicles in the mouse ovary: their development, physiological functions and implications for future research. *Mol Hum Reprod*. 2014;20:286–292.
91. **Zheng W, Zhang H, Gorre N, Risal S, Shen Y, Liu K.** Two classes of ovarian primordial follicles exhibit distinct developmental dynamics and physiological functions. *Hum Mol Genet*. 2014;23:920–928.
92. **Hummitzsch K, Irving-Rodgers HF, Hatzirodos N, et al.** A new model of development of the mammalian ovary and follicles. *PLoS One*. 2013;8:e55578.
93. **Rastetter RH, Bernard P, Palmer JS, et al.** Marker genes identify three somatic cell types in the fetal mouse ovary. *Dev Biol*. 2014;394:242–252.
94. **Gundra UM, Girgis NM, Ruckerl D, et al.** Alternatively activated macrophages derived from monocytes and tissue macrophages are phenotypically and functionally distinct. *Blood*. 2014;123:e110–e122.
95. **Mullany LK, Fan HY, Liu Z, et al.** Molecular characterization of ovarian surface epithelial cells transformed by KrasG12D and loss of Pten in a mouse model in vivo. *Oncogene*. 2011;30:3522–3536.
96. **Richards JS, Jahnsen T, Hedin L, et al.** Ovarian follicular development: from physiology to molecular biology. *Recent Prog Horm Res*. 1987;43:231–276.
97. **Richards JS, Pangas SA.** The ovary: basic biology and clinical implications. *J Clin Invest*. 2010;120:963–972.
98. **Chu S, Rushdi S, Zumpe ET, et al.** FSH-regulated gene expression profiles in ovarian tumours and normal ovaries. *Mol Hum Reprod*. 2002;8:426–433.
99. **Risma KA, Hirshfield AN, Nilson JH.** Elevated luteinizing hormone in prepubertal transgenic mice causes hyperandrogenemia, precocious puberty, and substantial ovarian pathology. *Endocrinology*. 1997;138:3540–3547.
100. **St John MA, Tao W, Fei X, et al.** Mice deficient of Lats1 develop soft-tissue sarcomas, ovarian tumours and pituitary dysfunction. *Nat Genet*. 1999;21:182–186.
101. **Pisarska MD, Kuo FT, Bentsi-Barnes IK, Khan S, Barlow GM.** LATS1 phosphorylates forkhead L2 and regulates its transcrip-

tional activity. *Am J Physiol Endocrinol Metab*. 2010;299:E101–E109.
102. **Bentsi-Barnes IK, Kuo FT, Barlow GM, Pisarska MD.** Human forkhead L2 represses key genes in granulosa cell differentiation including aromatase, P450scc, and cyclin D2. *Fertil Steril*. 2010; 94:353–356.
103. **Durlinger AL, Visser JA, Themmen AP.** Regulation of ovarian function: the role of anti-Müllerian hormone. *Reproduction*. 2002;124:601–609.
104. **Visser JA, Schipper I, Laven JS, Themmen AP.** Anti-Müllerian hormone: an ovarian reserve marker in primary ovarian insufficiency. *Nat Rev Endocrinol*. 2012;8:331–341.
105. **Richards JS.** Hormonal control of gene expression in the ovary. *Endocr Rev*. 1994;15:725–751.
106. **Richards JS.** Perspective: the ovarian follicle–a perspective in 2001. *Endocrinology*. 2001;142:2184–2193.
107. **Prunskaite-Hyyryläinen R, Shan J, Railo A, et al.** Wnt4, a pleiotropic signal for controlling cell polarity, basement membrane integrity, and antimüllerian hormone expression during oocyte maturation in the female follicle. *FASEB J*. 2014;28:1568–1581.
108. **Vainio S, Heikkilä M, Kispert A, Chin N, McMahon AP.** Female development in mammals is regulated by Wnt-4 signalling. *Nature*. 1999;397:405–409.
109. **Ottolenghi C, Pelosi E, Tran J, et al.** Loss of Wnt4 and Foxl2 leads to female-to-male sex reversal extending to germ cells. *Hum Mol Genet*. 2007;16:2795–2804.
110. **Miyamoto N, Yoshida M, Kuratani S, Matsuo I, Aizawa S.** Defects of urogenital development in mice lacking Emx2. *Development*. 1997;124:1653–1664.
111. **Taylor HS, Fei X.** Emx2 regulates mammalian reproduction by altering endometrial cell proliferation. *Mol Endocrinol*. 2005;19: 2839–2846.
112. **Okamoto J, Kratz JR, Hirata T, et al.** Downregulation of EMX2 is associated with clinical outcomes in lung adenocarcinoma patients. *Clin Lung Cancer*. 2011;12:237–244.
113. **Bilandzic M, Chu S, Farnworth PG, et al.** Loss of betaglycan contributes to the malignant properties of human granulosa tumor cells. *Mol Endocrinol*. 2009;23:539–548.
114. **Bilandzic M, Chu S, Wang Y, et al.** Betaglycan alters NFκB-TGFβ2 cross talk to reduce survival of human granulosa tumor cells. *Mol Endocrinol*. 2013;27:466–479.
115. **Lewis KA, Gray PC, Blount AL, et al.** Betaglycan binds inhibin and can mediate functional antagonism of activin signalling. *Nature*. 2000;404:411–414.
116. **Pangas SA.** Regulation of the ovarian reserve by members of the transforming growth factor β family. *Mol Reprod Dev*. 2012;79: 666–679.
117. **Parma P, Radi O, Vidal V, et al.** R-Spondin1 is essential in sex determination, skin differentiation and malignancy. *Nat Genet*. 2006;38:1304–1309.
118. **Bittinger S, Alexiadis M, Fuller PJ.** Expression status and mutational analysis of the PTEN and PI3K subunit genes in ovarian granulosa cell tumors. *Int J Gynecol Cancer*. 2009;19:339–342.
119. **Mullany LK, Liu Z, Wong KK, et al.** Tumor repressor protein 53 and steroid hormones provide a new paradigm for ovarian cancer metastases. *Mol Endocrinol*. 2014;28:127–137.
120. **He CH, Lee CG, Dela Cruz CS, et al.** Chitinase 3-like 1 regulates cellular and tissue responses via IL-13 receptor α2. *Cell Rep*. 2013; 4:830–841.
121. **Libreros S, Garcia-Areas R, Iragavarapu-Charyulu V.** CHI3L1 plays a role in cancer through enhanced production of pro-inflammatory/pro-tumorigenic and angiogenic factors. *Immunol Res*. 2013;57:99–105.
122. **Liu L, Rajareddy S, Reddy P, et al.** Infertility caused by retardation of follicular development in mice with oocyte-specific expression of Foxo3a. *Development*. 2007;134:199–209.